NASA

Technical Memorandum 78097

(NASA-TM-78097) OSO-8 X-RAY SPECTRA OF CLUSTERS OF GALAXIES. 1. OBSERVATIONS OF TWENTY CLUSTERS: PHYSICAL CORRELATIONS (NASA) 55 p HC A04/MF A01 CSCL 03A G3/89

N78-20030

Unclas 08728

OSO-8 X-Ray Spectra of Clusters of Galaxies. 1. Observations of Twenty Clusters: Physical Correlations

R. F. Mushotzky, P. J. Serlemitsos, B. W. Smith, E. A. Boldt and S. S. Holt

MARCH 1978

National Aeronautics and Space Administration

Goddard Space Flight Center
Greenbelt, Maryland 20771

OSO-8 X-RAY SPECTRA OF CLUSTERS OF GALAXIES.

I. OBSERVATIONS OF TWENTY CLUSTERS; PHYSICAL CORRELATIONS

R.F. Mushotzky*, P.J. Serlemitsos, Barham W. Smith**,
E.A. Boldt, and S.S. Holt

Laboratory for High Energy Astrophysics
NASA/Goddard Space Flight Center
Greenbelt, Maryland 20771

ABSTRACT

OSO-8 X-ray spectra from 2 to 20 keV have been analyzed for 26 clusters of galaxies. For 20 clusters we present temperatures, emission integrals, iron abundances, and low energy absorption measurements. Our data give, in general, better fits to thermal bremsstrahlung than to power law models. Eight clusters have positive iron emission line detections at the 90% confidence level, and all twenty cluster spectra are consistent with Fe/H = 1.4×10^{-5} by number with the possible exception of Virgo. Thus we confirm that X-ray emission in our energy band is predominantly thermal radiation from hot intracluster gas rather than inverse Compton radiation.

Physical correlations between X-ray spectral parameters and other cluster properties are examined. We find that: (1) the X-ray temperature is approximately proportional to the square of the velocity dispersion of the galaxies, (2) the emission integral and therefore the bolometric X-ray luminosity is a strong function of the X-ray temperature, (3) the X-ray temperature and emission integral are better correlated with cluster central galaxy density than with richness, (4) temperature and emission

*NAS/NRC Research Associate
**Also Dept. of Physics and Astronomy, Univ. of Maryland

integral are separately correlated with Rood-Sastry type, and (5) the fraction of galaxies which are spirals is correlated with the observed ram pressure in the cluster core. The physical implications of this data are discussed.

I. INTRODUCTION

Spectra of X-ray sources identified with clusters of galaxies (e.g. Gursky et al. 1972) which have been obtained from gas proportional counters have been particularly useful in our understanding of the nature of this emission. This understanding has been aided by the steady fluxes from these sources, their relatively simple continua, and the presence of iron emission lines in an energy band which allows proportional counter resolution to identify them unambiguously. Spectral observations reported to date include, for the most part, those of the strongest cluster sources (e.g. Kellogg, Baldwin, and Koch 1975; and Mitchell et al. 1976); together with spatially resolved observations, they strongly favor a thermal origin for the radiation in a hot intracluster gas, with at least some contribution to the gas from the galaxies themselves (see Lea 1977 for a recent review).

The Goddard Space Flight Center Cosmic X-ray Spectroscopy experiment aboard the OSO-8 observatory has now covered 26 cluster sources, allowing us to conduct a more comprehensive study. We concentrate on the determination from spectra of physical parameters such as X-ray temperatures, emission integrals, and luminosities corrected for spectral shape, which are given here for 20 of our sources, a large sample (about 40%) of the known cluster sources. We are able to conduct tests on 1) correlations between X-ray, optical, and radio properties of clusters, 2) the universal iron abundance hypothesis (Serlemitsos et al. 1977), 3) whether the observed low energy absorption is due entirely to material in our galaxy, and 4) the contribution of individual galaxies to the X-ray emission.

II. INSTRUMENTATION AND DATA COLLECTION

These observations were performed with three separate mechanically collimated proportional counters on board the OSO-8 satellite, comprising the Goddard Cosmic X-ray Spectroscopy Experiment (CXS). The A detector is a 263 cm^2 xenon counter with a 5^o FWHM circular field of view. It is canted 5^o to the negative spin axis and scans an annulus on the sky once every spacecraft rotation period ($\sim$ 10 s), so that source and background pulse height spectra are accumulated concurrently. This detector has an energy resolution of about 18% at 6 keV. The gain and detector resolution have been determined using an onboard Am^{241} source, and the energy calibration is accurate to $\sim$ 1%. The C detector is a pointed 234 cm^2 xenon counter with a propane-neon electron rejection layer in front of the main counter volume. The 5^o FWHM field of view looks along the positive spin axis of the spacecraft. The B detector is a 37 cm^2 argon counter with an energy resolution of about 17% at 6 keV. The 3.34^o FWHM field of view looks along the negative spin axis. Background observations for the B and C detectors are made when there are no known sources in the field of view during times as close as possible to the actual observations. For a more detailed description of the OSO-8 CXS experiment see Pravdo (1977).

Since the mode of observations is essentially pointed, there are varying exposures for the sources analyzed in this paper. Our longest cluster observation is $\sim 8.5 \times 10^6$ cm^2 s with the B detector for the Perseus cluster, and our shortest is $\sim 7 \times 10^5$ cm^2 s with the C detector for Abell 1060. Only data which pass stringent criteria for absence of electron contamination are used for analysis of source spectra. Some observations are further restricted by source confusion.

III. OBSERVATIONS AND DATA ANALYSIS

The clusters of galaxies selected for analysis in this paper are chosen from the list of Gursky and Schwartz (1977) which is based on UHURU data and from identifications in the Ariel 2A catalog of high latitude X-ray sources (Cooke et al. 1977). All of their positional coincidences for which OSO-8 data were available prior to August 1977 were analyzed, consistent with restrictions already mentioned. Although sky coverage by our experiment is not uniform, we feel that this sample is representative of the X-ray sources which have been associated with clusters of galaxies based on the 3U and 2A surveys. We have not yet undertaken a comparable study of additional cluster sources identified in the 4U catalog (Forman et al. 1977) or observed after the above date.

The spectral data were analyzed in the usual CXS manner (e.g. Pravdo et al. 1976). Model spectra were convolved through the detector response function and compared with pulse height data, and the model parameters were adjusted by the χ^2 test while normalizing on the total number of counts. We have fitted two models to the continuum emission: thermal bremsstrahlung and single power laws. In both cases the photoelectric cross sections of Brown and Gould (1970) as amended by Fireman (1974) were used to model absorption of the X-ray spectrum within our galaxy. In the thermal case only, we have included an emission line feature at the energy appropriate to the temperature derived from the continuum (6.7 to 6.9 keV, see below) and shifted by the optical redshift of the cluster, if known. The lines were assumed to be intrinsically narrow (<< resolution), consistent with collisional excitation of highly ionized iron ions in a hot gas.

For Fe XXV a strong line feature from n = 2 to n = 1 transitions occurs at $\sim$ 6.7 keV, while for Fe XXVI the dominant feature (Lyman α) appears at $\sim$ 6.95 keV. If a line was required to fit a source spectrum with more than 90% confidence, a separate determination of the best-fitting line energy was made.

In Figure 1 we show 8 representative photon spectra derived from the best thermal fits to our pulse height spectra. The sources in Figure 1a were observed with relatively high exposure and exhibit definite iron lines, while those in Figure 1b were observed with relatively low exposure. These figures indicate the range of statistical significance of our data.

To generate 90% confidence expected errors for the joint estimation of model parameters, the prescription of Lampton, Margon, and Bowyer (1976) was employed. For example, in our preferred (thermal) model containing temperature, absorbing column density, and iron line strength as free parameters we quote the limits of a rectangular box in 3-dimensional parameter space which fully encloses the 90% confidence contour determined from χ^2. In most cases the 90% joint confidence interval for each parameter is considerably larger than the 68% (χ^2 + 1) interval for the independent error on one parameter (Avni 1976). Table 1 shows the difference between the parameter spaces enclosed for three representative clusters.

It should be noted in passing that because our field of view exceeds all known cluster sizes, we have measured the spatially integrated total spectrum and not that of some restricted portion of each cluster.

IV. RESULTS

We aim, of course, to distinguish between various models which have been proposed to explain X-ray emission from clusters of galaxies. Our results favor radiation from a hot intracluster gas in collisional equilibrium, for which we expect an optically thin thermal bremsstrahlung continuum and perhaps an iron emission line. Although more sophisticated thermal models are possible (e.g. Lea 1977), we have fitted only isothermal models in this paper to preserve the uniformity of treatment throughout our sample. All thermal bremsstrahlung calculations in this paper include hydrogen and helium, with He/H = .085 by number, and use accurate Gaunt factors (Kellogg, Baldwin, and Koch 1975). A second model, inverse Compton scattering of the microwave background by relativistic electrons, should produce power law X-ray spectra. Since the presence of a narrow iron line feature is extremely difficult to understand in models where the inverse Compton process produces the X-ray continuum, we have not allowed power law fits with lines. A third model has been proposed, viz. radiation from some distribution of compact X-ray sources, which would produce a complex composite spectrum (Katz 1976; Fabian et al. 1976).

In the first two cases there should be negligible self-absorption of lower energy X-rays within the source. However, the multiple-compact-source model predicts a spectrum having characteristics of galactic binary sources (e.g. a low energy turnover and considerable temporal variability). While the temporal variability may be obscured by integrated observations of the source distribution, the general absence of the implied low-energy turnover in our sample of cluster spectra has dissuaded us from attempting

to fit spectral models representing the third case to our data.

As Culhane (1977) has again pointed out, it is in general quite difficult to decide between thermal and nonthermal models solely on the basis of 2 - 10 keV spectra with limited statistics from proportional counters. However, with our roughly 2 - 20 keV band we find our statistics adequate to distinguish between the two simple models for an appreciable fraction of our sample. We shall break down our discussion into three parts: the continuum, the low energy turnover, and the iron emission line.

A. The Continuum

In Table 2 we present the results of our spectral fits. In column 1 we give the X-ray source position which has been assumed in calculating the true flux from the source, in column 2 we give the name of the cluster with which the source is believed to be associated, and in column 3 we note the detectors used and their exposure to the source. Columns 4 through 8 give the best thermal fit with errors, respectively listing kT in keV, N_H in cm^{-2}, the equivalent width of the iron feature in keV, the assumed energy of the iron feature (derived from kT and redshift), and the minimum χ^2 per degree of freedom (33 degrees of freedom, usually). In addition, for line features inconsistent with zero equivalent width at the 90% confidence level, a separate determination of the best fitting line energy is made and the result is also quoted in column 7 with a one-parameter, $\chi^2_{min} + 1$ error. Columns 9 through 11 list, for power law fits, the photon spectral index, N_H, and χ^2_{dof} (34 degrees of freedom, usually).

Over our sample of 20 objects, isothermal bremsstrahlung spectra including an iron emission feature provide more acceptable fits than power

law spectra. It is true that both types of fit are acceptable (χ^2 per degree of freedom < 1.5) except for the strongest sources with the best statistics above 10 keV. Yet if most clusters truly had nonthermal spectra, it is highly unlikely that thermal models with narrow line features would provide significantly better fits for 9 out of 20 sources while a power law provided a significantly better fit in only two cases. We feel that this constitutes new evidence that cluster spectra are predominantly thermal.

The measured cluster temperatures range from 2 to over 20 keV with most values between 4 and 10 keV. This study would have missed clusters with very low temperatures (kT < 2 keV) due to the 2-10 keV bandwidth of the surveys used to select the cluster candidates. However, because there is no such effect for kT > 10 keV, we conclude that the lack of many clusters with such high temperatures is real. This may be no surprise in view of the observed distribution of cluster velocity dispersions (Smith et al. 1978a).

Several of our sources merit special attention because of exceptionally good statistics or because of spectral peculiarities. It is to be expected that the spectra with the smallest statistical errors require more detailed models than we discuss here. Perseus, Coma, and Virgo cannot be adequately fit by either single temperature bremsstrahlung with a 6.7 keV iron line or by a single power law. We include here the best fitting parameters for these simple models in order to show their membership in the larger class of sources (with poorer statistics) that we are discussing. More detailed fits to Perseus, Coma, and Virgo will be described in a subsequent

paper (Smith et al. 1978b). It should be clear therefore that we do not claim that cluster spectra are exactly isothermal with a single iron line feature: Fitting all of our sources with models using the additional parameters required for the three strongest sources is not warranted by the data. However, more detailed fits to Perseus, Coma, and Virgo do not contradict any of the conclusions presented in this paper.

We were unable to adequately fit 3U1555+27, identified with Abell 2142, using a thermal bremsstrahlung model with kT < 30 keV. As the only object in our sample requiring a very high temperature or a power law model, it might be considered in a different class. This source exhibits evidence for iron line emission at the 90% confidence level. A line in A2142 would not be expected from kT > 30 keV gas. We suggest that A2142 may be similar to Virgo with both high (kT > 20) and low temperature regions present or with a strong power law component.

B. Low Energy Absorption

As noted above, neither thermal bremsstrahlung from intracluster gas nor inverse Compton radiation predict any low energy absorption within the source. In Table 3 we give the atomic hydrogen column densities N_H due to material in our galaxy along the lines of sight to our sources from Heiles (1976), which can be compared to the measured values in Table 2. It should be noted that multicomponent spectral models having low energy excesses would require additional absorption. Only five of the thermal spectra have N_H significantly larger than the Heiles value at the 90% confidence level, as do a similar percentage of the power law fits (in general, power law fits require more absorption than thermal fits). The

five clusters having significant absorption in thermal model fits are 3C129, Abell 401, Coma, Perseus, and Abell 1367.

In the case of the 3C129 cluster, which lies almost directly in the galactic plane in the anticenter direction, we expect to see absorption similar to that in the Crab nebula. Spinrad (1976) gives $E_{B-V} \sim 0.9$ for the galaxy 3C129, which implies $N_H \sim 6.7 \times 10^{21}$ cm^{-2} using the conversion factor of Ryter, Cesarsky, and Audouze (1976). This agrees well with our data for both 3C129 and the Crab nebula as measured by the CXS experiment.

For Abell 401 our lower limit is $N_H > 9 \times 10^{20}$ cm^{-2} which apparently excludes the Heiles value of 10^{20} cm^{-2}. For the Coma cluster our lower limit is 2.7 times the Heiles value and for the Perseus cluster it is 2.5 times the Heiles value. However, this situation is best discussed in the light of more detailed spectral fits (Smith et al. 1978b), as absorption values derived from simple models yielding unacceptable fits should be treated with caution. Kellogg, Baldwin, and Koch (1975) find $N_H \sim (6 \pm 1.5) \times 10^{21}$ cm^{-2} for Coma ($\chi^2_{min} + 1$ errors) which lies within our error bars. Malina et al. (1977) find $N_H < 2 \times 10^{21}$ for Perseus and $N_H < 5 \times 10^{21}$ for Coma.

For Abell 1367 we find a reduction in χ^2 from 32.9 to 24.9 (for 33 d.o.f.) when absorption is added as a free parameter. This is not significant at the 3σ level. However, it could be taken as evidence that a significant amount of the X-ray flux comes from 3C264. We also note that there is a possibly significant factor-of-two variation between the OSO-8 and 4U catalog 2 - 6 keV fluxes for this source.

In summary, we conclude that sources identified as clusters of galaxies have much less intrinsic low energy absorption than compact sources, agreeing well with thermal bremsstrahlung models.

C. Iron Line Emission

We have interpreted the equivalent widths in Table 2 in the following way. Assuming that collisional (coronal) equilibrium in a low density plasma applies to the intracluster medium and that the continuum and line emission arise in the same gas, one can calculate the expected intensities and energy centroids for the iron line blend from the observed continuum temperature for one value of the iron abundance. The observed equivalent width then determines the actual iron abundance:

$$\left(\frac{Fe}{H}\right)_{observed} = \frac{(E.W.)\ observed}{(E.W.)\ expected} \left(\frac{Fe}{H}\right)_{assumed} \qquad (1)$$

We have used the line intensities of Raymond and Smith (1977), who base their work on their new calculation of the ionization equilibrum using collisional ionization rates given by Summers (1976). Rates for the 6.7 and 6.9 keV iron lines are from Mewe (1972), but Raymond and Smith have adjusted Mewe's Gaunt factors to agree better with the calculations of Jones (1974) and Bhalla et al. (1975). They have included contributions to the line blend from dielectronic recombinations and inner shell excitations of other ions (satellite lines). They have also added the contributions of cascades from higher levels in hydrogen- and helium-like ions. The helium abundance assumed has been explicitly noted above, since it affects the equivalent width through its $\sim$ 35% contribution to bremsstrahlung. Using the Raymond and Smith calculation, we plot in Figure 2a the total

equivalent width of the 6.7 - 6.9 keV line blend as a function of temperature, for two values of the iron abundance.

In Figure 2a we also plot the equivalent width for the seven clusters in which it is best determined. All these points except Virgo are consistent with the dashed curve, i.e. with a single value of the iron abundance. This consistency is more easily seen in Figure 2b, which shows the iron-to-hydrogen ratios derived from all the usable equivalent width measurements in Table 2. The errors for Abell 1060 and Abell 2589 are too large to constrain models for these clusters. The plotted values of Fe/H are almost all within 1σ of the weighted average value:

$$\frac{Fe}{H} \quad \sim \quad (1.4 \pm .1) \quad x \quad 10^{-5}, \qquad (2)$$

which is the abundance chosen for the dashed curve in Figure 2a, and which is roughly half the solar value.

There is no obvious trend in the data points of Figure 2b, which implies that the line intensities and continua are indeed related as the collisional equilibrium theory predicts. This fact argues in favor of the hot intracluster gas hypothesis. Similarly, it argues against associating the iron emission with individual galaxies (unless the continuum emission comes from the same galaxies, in conflict with spatially resolved observations to date) or with compact objects (whether binary stars or active galactic nuclei) where this relation between iron intensity and overall spectrum is not expected.

It is interesting that none of the 90% confidence upper limits exclude the abundance found for the Perseus cluster, which has the smallest error

in Fe/H. Eight clusters of galaxies have a nonzero iron abundance at the 90% confidence level, viz. Perseus, Coma, Virgo, 3C129, Abell 347 (?), Centaurus, SC1251-28, and A1060. The abundance for Virgo is difficult to pin down because of the complexity of its spectrum; the value given is an approximation based on the assumption that all of the iron emission is due to the low temperature component. Mitchell and Culhane (1977) have also observed an iron line in the Centaurus cluster; their line intensity is about twice as large, but our error bars overlap at the 90% level. Abell 1060 technically has a nonzero iron abundance at the 90% level in our data (not surprisingly as there is a large equivalent width predicted for its temperature) but the errors are large.

All of the observed energies of the iron line features are consistent with the expected energies, when the slight variation of the line blend centroid energy with temperature and the optical cluster redshifts are included. Conversely, the clusters with large optical redshifts and good X-ray statistics (e.g. SC1251-28) have line energies in good agreement with their redshifts.

We have two or more independent observations for a number of clusters, either with different detectors or at different times or both. In these cases we do not observe any significant variation in the iron line intensity. In contrast, time variability of iron line features has been observed in galactic X-ray sources (e.g. Boldt 1977).

We conclude that our data are consistent with one iron abundance for all clusters of galaxies except Virgo and A2142.

D. Fluxes, Luminosities and Emission Integrals

In Table 4, column 1, we present the values of the actual flux observed at the detector for one value of the energy, 5 keV, which can be used as a normalization to extrapolate our spectra to any desired energy. For single temperature bremsstrahlung we can calculate the emission integral $\langle n_e n_H \rangle V$ from the flux (n_e is the electron number density, n_H is the total hydrogen density, and V is the volume of the emission region). We have derived distances from optical redshifts using a Hubble constant H_o = 55 km s^{-1} Mpc^{-1}. Values of $\langle n_e n_H \rangle V$ appear in column 2 of Table 4. In columns 3 and 4 we give the 2 - 6 keV and 2 - 10 keV luminosities integrated directly from our best fit thermal spectra. The iron features do not contribute significantly to these luminosities. In column 5 we give the bolometric bremsstrahlung luminosity obtained from

$$L_{bol} \approx \sum_{i=H,He} 1.43 \times 10^{-27} \langle n_e n_i \rangle V \; Z_i^2 \, \bar{g}(T,Z_i) T^{\frac{1}{2}} \text{ erg s}^{-1}$$
$$\approx 7.7 \times 10^{-24} \langle n_e n_H \rangle V \; T_{keV}^{\frac{1}{2}} \text{ erg s}^{-1} \qquad (3)$$

where $\bar{g}$ is the energy-averaged bremsstrahlung Gaunt factor from Karzas and Latter (1961). We see that, particularly for clusters whose temperature is outside the range 3 - 10 keV, the bolometric luminosity differs from the UHURU or Ariel band luminosity in a way not predictable from the band luminosity alone.

Values of the emission integral cover over two orders of magnitude, but most clusters fall near 10^{68} cm^{-3}. We find in § V.A.iii that there is a tendency for clusters with low temperatures to have small emission

integrals, and therefore particularly low luminosities. Such clusters cannot be observed at very great distances in a flux-limited survey (cf. Schwartz 1977). Therefore our distribution of emission integrals, just like our distribution of temperatures, should be corrected for selection effects to make it representative of all clusters.

E. The Absence of Time Variability

X-ray sources in clusters of galaxies should not vary in time on scales $\lesssim 10^9$ years if their emission is principally due to thermal bremsstrahlung from a hot intracluster medium. It is well known (e.g. Forman, Jones, and Tananbaum 1976) that all strong galactic X-ray sources are time variable with the exception of supernova remnants. Thus for sources without well determined positions a strong discriminant between cluster sources and high latitude galactic sources is the absence or presence of variability.

We have two independent tests of time variability available: First, we can plot our own data on time scales of days or, on those few occasions when we observed a source a second time, years. Second, we can compare our OSO-8 flux to the UHURU or Ariel 5 flux in the appropriate band.

In Figure 3 we show typical light curves for sources at different levels of OSO-8 exposure. Our interval checks show no significant variability of flux. However, for the source identified with Abell 1254 our data indicate either more than one source in the field of view or time variability. Since this source is labeled confused in the 2A catalog we do not conclude that it is variable. For our complete sample of sources identified with clusters, it seems unlikely that any large ($\gtrsim$ 30%) flux variations are

common, since a 1.5 UHURU count source is a 3σ detection in 10^3 seconds of observation with the A detector.

In comparing OSO-8, Ariel 5, and UHURU fluxes, care must be exercised in evaluating the methods by which they were determined. The OSO-8 fluxes are sums over all available data corrected for detector angular and energy response for the particular shape of the best-fitting spectrum. The UHURU and Ariel 5 fluxes have not been corrected for energy response to a spectral shape; probably this effect is under 30%. Moreover, the 4U catalog lists averages over the positive sightings of a source, a procedure which can overestimate the strength of a steady weak source and underestimate the error. Nevertheless we find fairly good agreement in Figure 4 between fluxes from the three experiments. We note that the scatter in the OSO-8 vs. 4U correlation becomes large below 3.5 UHURU counts. Again, the scatter in the OSO-8 vs. 2A correlation is larger than one would expect from statistics alone and there is a possible zero offset of ∿ .15 Ariel ct also noted by Warwick and Pye (1978). We do not know the exact sources of these discrepancies, but even if we ascribe them to variability of the sources, the variability is small. In view of the possible underestimation of errors, we feel that the 4U and 2A fluxes agree with OSO-8 fluxes. With essentially no evidence for time variability on scales of days or years, we have further reason to believe we are dealing with spatially extended sources.

F. Weak Detections and Upper Limits

We summarize in Table V the results for 6 probable clusters included in our survey which had either weak detections or upper limits. Errors are 1σ unless otherwise noted. Our fluxes do not disagree strongly with

the cataloged fluxes for any of these sources, when the probable systematic error on weak 4U source fluxes is taken into account. From our data we cannot comment on the accuracy of the identifications of these weak sources from either spectral or flux constancy data.

V. OBSERVATIONAL CORRELATIONS

The uniformity of analysis of these data uniquely qualify our sample for testing correlations between X-ray spectral properties and optical or radio properties of clusters of galaxies. We have not only tested correlations studied by other workers but have also searched for new correlations predicted by various theories. Most of this section deals with thermal models, but we discuss one correlation predicted by the inverse Compton model. In Table III we present the values of useful optical and radio parameters that we have adopted from the literature, allowing the reader to consider correlations that we do not include in this communication.

A. Thermal Bremsstrahlung Models

There are many possible correlated quantities in thermal models, and we have only considered what we believe to be a plausible subset for test purposes. We consider mostly correlations involving the temperature of the X-ray continuum and the emission integral with various non-X-ray properties. Since our values for the iron abundance in different clusters are consistent with one another, we are unable to investigate possible correlations with it.

(i) Velocity Dispersion vs. Temperature

In Figure 5 we plot the one-dimensional central velocity dispersion Δv_c against the measured X-ray temperature. Most published

velocity dispersions for clusters of galaxies are "mean" values, while we wish to make contact with the relation

$$\frac{GM_c}{a} = 3(\Delta v_c)^2 \qquad (4)$$

where M_c is the core virial mass and a is the core radius in the model gravitational potential of King (1972). Rood et al. (1972) show that for a King model fit to the Coma cluster, Δv_c is about 20% larger than the mean dispersion. This also seems to fit the velocity data for the Perseus cluster (Chincarini and Rood 1971). Therefore we have multiplied the published values of Δv (Table 3) by 1.2 before plotting them in Figure 5.

There is a strong correlation between Δv_c and the X-ray temperature. The regression coefficient assuming equal weights for the points in Figure 5 is r = .78 which is significant at the 99.5% level. However, if we fit a power law of the form $kT = A\,\Delta v_c^{\alpha} + B$, we find $\chi^2_{d.o.f.} = 5.2$, a very poor fit, with $\alpha = 0.94 \pm .25$. Therefore we have tried excluding clusters with dominant galaxies, i.e. those of Rood - Sastry types cD or B. Now the regression coefficient is r = .927 which for six data points has the same significance as that of the full data set, but the power law fit gives

$$\alpha = 1.6 \pm .3 \qquad (5)$$

with $\chi^2_{d.o.f.} = 1.50$. Considering only clusters with dominant galaxies, r = .43 which for four data points means less than 50% probability for a correlation. The power law fit has $\alpha = -.33 \pm .50$ with $\chi^2_{d.o.f.} = 3.1$. Thus while there is a probable correlation between Δv_c and kT for all

clusters, it does not seem to hold as strongly for clusters with dominant galaxies. However, because of the small sample sizes these correlations are subject to possible sampling and statistical error. Clearly, more velocity dispersion data are necessary to fully test the validity of the kT vs. $(\Delta v_c)^2$ relation.

Where a correlation exists, one may attempt to understand theoretically the observed values of the slope and intercept of the power law. The most general analytic models for the structure of intracluster atmospheres are polytropes (e.g. Lea 1977). In terms of the polytropic index γ one can describe the overall temperature and density structure of a cluster atmosphere, or approximate the structure resulting from more complex models. In the following paper (Smith et al. 1978a), we show how our spectra may be interpreted to give effective values of the polytropic index, but we quote the result here. All the data in Figure 5 determine a line $kT \propto \Delta v_c^2$ which implies $\gamma \tilde{\sim} 1.1$, indicating that a nearly isothermal ($\gamma = 1$) structure is suitable for the cluster sample taken as a whole. However, if gas falls from a large radius into the core under the influence of the core mass only, it acquires a gravitational temperature, $kT_G \tilde{\sim} GM_c/5a$, where we have included the work done in compressing the gas. Using equation (4) we can relate T_G to $(\Delta v_c)^2$. Perhaps, by coincidence, this gives the same line as drawn in Figure 5 corresponding to $\gamma \sim 1.1$ polytropic models.

(ii) Luminosity and Emission Integral vs. Temperature

Since the bolometric bremsstrahlung luminosity is proportional to $T^{\frac{1}{2}} \langle n_e n_H \rangle V$, we would not expect to recover a simple

$L \propto T^{\frac{1}{2}}$ relation in an L_{bol} vs. kT plot unless the values of $\langle n_e n_H \rangle V$ were independent of temperature. In Figure 6 we remove $T^{\frac{1}{2}}$ and show the emission integral vs. kT. The data have a correlation coefficient $r = .70$, significant at the 99% level, and a power law fit $\langle n_e n_H \rangle V \propto T^{\alpha}$ yields $1.6 \lesssim \alpha \lesssim 5.1$ with unacceptable χ^2.

This systematic trend, for hotter clusters to have larger emission integrals, is not simply a reflection of their larger virial mass. To see this, recall the common assumption that the mass of gas M_{gas} in clusters is a constant fraction of their core virial mass M_c. Since $M_c \propto \Delta v_c^2 a$, $M_c \propto Ta$. The mean gas density would then be $\langle n \rangle \propto Ta/V$, whence $\langle n_e n_H \rangle V \propto f T^2 a^2/V$, where f is a clumping factor representing the overall condensation of the gas, $f \equiv \langle n^2 \rangle / \langle n \rangle^2$. This would predict $\alpha' \sim 2$. This analysis leaves us with at least two possibilities for the interpretation of our stronger temperature dependence of the emission integral. First, preserving the assumption that $M_{gas} \propto M_c$, we must have $fa^2/V \propto T^{\delta}$ where $-0.4 \lesssim \delta \lesssim 3.1$ which implies that hotter clusters are more centrally condensed. The second alternative is to relax that assumption and to conclude that clusters with larger virial masses and thus higher temperatures gather proportionately larger masses of intracluster gas than smaller clusters. The low temperature clusters like Virgo have been observed previously to have proportionately less gas than more luminous clusters, so that the cluster gas may have become associated with massive galaxies like M87 alone (Bahcall and Sarazin 1977, Gorenstein et al. 1977).

(iii) Galaxy Densities vs. kT and $\langle n_e n_H \rangle V$

Abell's (1958) richness class R and Bahcall's (1977a) central galaxy density $\overline{N}_o$ are both based on counts of galaxies in a circular field around the cluster center. Since R represents a count within an Abell radius ($\sim$ 3 Mpc if H_o = 55 km $s^{-1}Mpc^{-1}$), it should include most galaxies in the cluster. However, the richness criterion has limitations: First, the integers 0 to 4, for X-ray clusters, are not a very quantitative measure of galaxy density; secondly, R is not a linear function of the actual galaxy density; and finally, as explained in Abell (1958), the richness classes were defined to reflect the expected precision of the counts (i.e. differences of one class are not always significant). In contrast, Bahcall's $\overline{N}_o$ seems to be a more precise count of galaxian density, to fainter limiting magnitude, within a radius of 0.5 Mpc, which for most clusters is about twice the core radius of the galaxy distribution (cf. Bahcall 1975). This radius is well chosen, because most of the X-ray emission above 2 keV in clusters of galaxies is both observed (Kellogg and Murray 1974) and expected to come from a region of about this size. With this in mind, we are not surprised to find that $\overline{N}_o$ correlates much more tightly with X-ray properties of clusters than does the richness R (cf. Jones and Forman 1977). To see that the two measures of galaxy density are indeed different, one need only try correlating $\overline{N}_o$ and R for the clusters in Bahcall (1977a): For example, among richness 2 clusters, $14 \leq \overline{N}_o \leq 35$, a very wide range.

When both galaxy densities are plotted against X-ray temperature (Fig. 7) for those clusters in our sample with available data, we find

no significant correlation of R with kT, while for $\overline{N}_o$ vs. kT we find r = .79, a virtually certain correlation (> 99.5%). Fitting a power law to the latter data, we find $kT \propto \overline{N}_o^{\alpha}$ with $\alpha = 1.0 \pm .15$. This linear relation is expected if $kT \propto \Delta v_c^2$ and if the density of counted galaxies $\overline{N}_o$ is proportional to the true central virial mass density (cf. Bahcall 1977a). This is further evidence that kT is related to the depth of the gravitational potential. Since $\overline{N}_o$ is more easily and accurately measured than the velocity dispersion, perhaps the above evidence is stronger than that given in §i. It is unclear whether R fails to correlate: 1) because it is poorly measured, or 2) because the X-ray temperature does not depend on the galaxy density inside the Abell radius but only on the galaxy density inside a few core radii. The latter reason is plausible if many clusters of galaxies are not yet dynamically relaxed, so that only the central galaxy density accurately corresponds to the depth of the potential.

When R and $\overline{N}_o$ are plotted against $\langle n_e n_H \rangle V$ (Figure 8a,b), the richness correlation is again weaker, having r = .37 (we have adopted Bahcall's values of R = 3 for SC1329-31 and SC1251-28, which were classified R = 0 by Lugger 1977). The $\overline{N}_o$ vs. $\langle n_e n_H \rangle V$ correlation, by contrast, has r = .82, again a virtually certain (>99.9%) correlation. The power law fit gives $\langle n_e n_H \rangle V \propto \overline{N}_o^{\beta}$ with $\beta \simeq 3 \pm .5$, where the error has been estimated. An $\langle n_e n_H \rangle V$ vs. $\overline{N}_o$ power law can also be derived by combining our $\langle n_e n_H \rangle V$ vs. kT and kT vs. $\overline{N}_o$ relations, given above. The result is $\langle n_e n_H \rangle V \propto \overline{N}_o^{\beta}$ with $2.8 \lesssim \beta \lesssim 5.2$ which is consistent with the result from the direct correlation within errors. This is slightly too large a power to fit with the simplest assumptions, namely $\langle n \rangle \propto \overline{N}_o$ and V = const, and requires

that the product fV increase somewhat with $\overline{N}_o$, where f is defined in §i.

iv) Cluster Morphology and Spiral Fraction

Recently Bahcall (1977a,b) has claimed strong correlations for X-ray clusters between optical morphology and X-ray luminosity. Specifically she found that clusters with dominant galaxies (Rood-Sastry types cD and B) were more luminous in X-rays, on the average, than clusters of more distributed optical morphology (RS types C, F, and I). Also, she found that clusters with larger X-ray luminosity have smaller fractions of spirals among their member galaxies.

Grouping the RS types along the linear sequence corresponding to central concentration, rather than as a "tuning fork" (Rood and Sastry 1971), we arrive at the four groups of Bahcall (1977a), viz. (cD,B); L; (C,F); and I. The unweighted average temperatures for these four groups, among the clusters in our sample are, respectively, 8.09, 6.9, 4.68, and 3.75 keV. For the purpose of this calculation we have excluded 3C129 which has an unknown type; A2142 (RS type B) which has kT > 30 keV, and A1254 (RS Type I) which is in a confused region. If A1254 is in fact the object associated with 2A1150+720, the average kT for irregular clusters is increased to 8.8 keV. Barring this, a trend is observed in temperature as a function of RS type. The correlation of emission integral with RS type is more dramatic (Figure 8c). The unweighted averages for the four groups defined above are, respectively, 14.6, 14, 4.8, and 0.75 x 10^{67} cm^{-3}, with the same exclusions as above. It is seen that the variation in $\langle n_e n_H \rangle$ V with RS type contributes more than that in kT to the variation of luminosity with RS type. In other words, centrally condensed clusters

have slightly higher X-ray temperatures than irregular clusters, but condensed clusters have much larger emission integrals; this agrees with the correlation between L_x and kT found in § ıı.

Turning to spiral fraction, we note that, in a model in which spiral galaxies are stripped of gas by ablation as they move through an intracluster medium, the mean ram pressure ρv_g^2 is proportional to ρkT. Here ρ is the mass density of intracluster gas and v_g, the galaxy velocity relative to the intracluster gas, is proportional on the average to the velocity dispersion. If this model is applicable to real clusters, we might expect a correlation between $Q \equiv (\langle n_e n_H \rangle V)^{\frac{1}{2}} kT$ and the mean ram pressure experienced by galaxies moving through the core, as measured by the fraction F(Sp) of galaxies in the cluster which are spirals. We assume (cf. Kellogg and Murray 1974) that most clusters have roughly the same V. This correlation (Figure 9) has r = .92 for a logarithmic fit, significant at more than the 99% level. Bahcall (1977b) suggests that $F \propto Q^{-1}$ if the observed spirals survive because they are too massive to be stripped by ram pressure, which is consistent with our result within experimental error.

B. Inverse Compton Models

In contrast to the many correlations we can search for in thermal models of cluster emission, there are few relationships in nonthermal models which are amenable to test with our data. However, X-ray emission by inverse Compton scattering of relativistic electrons off the 3K background radiation predicts a power law X-ray spectrum with an index approximately equal to the slope of the low frequency radio continuum, α_{LFR}. Using

Tables 2 and 3 we can compare the radio index from Erickson, Mathews, and Viner (1977) to the best fit power law X-ray index. Although the values are often comparable, the radio values (which we take to have negligible errors) lie within the 90% confidence error limits on the X-ray index only about half the time. The formal correlation coefficient between the two sets of indices is only r = .15, which indicates that these quantities have less than a 20% chance of a power law correlation.

If we assume that some fraction of the X-ray flux is due to Compton scattering of microwave photons off the relativistic particles producing the low frequency radio source, then the measured spectral index, α, X-ray flux F_{ν_x} and radio flux $F_{\nu r}$ (Felten and Morrison 1966) determine the only free parameter, the magnetic field H:

$$H = A_1 K (5.4 \times 10^4)^{\alpha - 1}{}^{(1/\alpha + 1)} \text{ gauss}, \qquad (7)$$

where $K = F_{\nu r}(\nu_o)/F_{\nu x}(\nu_o)$; $A_1 \sim 10^{-11}$ and ν_o is some fiducial frequency. Our data, combined with that of Erickson, Matthews and Viner (1977) leads to $2 \times 10^{-8} < H < 2 \times 10^{-7}$ gauss for all the clusters in our sample for which 26 MHz radio data exist. If we wish to account for only $\sim$10% of the X-ray flux by I-C scattering then $5 \times 10^{-8} \lesssim H \lesssim 6 \times 10^{-7}$. Thus it is quite easy to reduce the predicted I-C flux from known low frequency radio sources to an unmeasurable level by increasing H only slightly to $>10^{-7}$ gauss. For most cluster radio sources (Harris and Romanishin 1974) the equilibrium magnetic field has $4 \times 10^{-7} < H < 1.4 \times 10^{-6}$, in all cases considerably larger than the field required to account for even 10% of the 2-20 keV X-ray flux. We also note that the predictions of

Harris and Romanishin for the 10-20 keV flux from A401, A1367 and A2256 are at least a factor of 2 too large compared to our measured fluxes. We thus feel that certainly < 50% and probably < 20% of the 2-20 keV X-ray flux is due to I-C scattering. If the magnetic field of the cluster is near the equipartion value, the I-C flux will be larger than the thermal X-ray flux only at energies > 100 keV. Thus, as early papers have noted, the most sensitive test for I-C flux is at higher energies than those of our observations.

VI. CONCLUSIONS

A number of questions about the nature of cluster X-ray sources have been addressed in this paper: Is the X-ray emission process thermal or nonthermal? If thermal, is the emitting gas from galaxies or is it primordial? What is the heat source? What is the role of dominant galaxies and cluster morphology? Here we summarize the various parts of our answers to these questions, while a fuller discussion is left for the following paper.

We have presented a number of results for X-ray spectra of clusters in the 2-30 keV band which favor an interpretation of the spectra of thermal bremsstrahlung from hot intracluster gas. First, spectral fits to the X-ray continua are statistically better for bremsstrahlung than are power laws. A few clusters have such good counting statistics that nonthermal fits can be eliminated. Secondly, these thermal fits require little low energy absorption and are consistent with the optically thin models required by the extent of the X-ray regions. Thirdly, iron lines are common in cluster spectra and their energies and narrow intrinsic widths demand

a thermal interpretation. The distribution of line-to-continuum ratios is consistent with an origin for both lines and continuum in the same intracluster gas. Fourthly, the X-ray temperature correlates well with two measures of the gravitational potential in the cluster center: the central velocity dispersion of the galaxies and the central galaxy density. These correlations have a straightforward interpretation only if the X-rays come from a hot gas whose temperature reflects the potential energy transformed by some process into heat by cluster formation. Fifthly, the emission integral correlates with both the temperature and the central galaxy density, which again implies the presence of hot gas. Lastly, the spiral fraction is systematically smaller in clusters with larger density and higher temperature, as if hot gas were responsible. We feel that this paper and other work published recently (e.g. Mitchell et al. 1976; Bahcall 1977a,b; Gorenstein et al. 1977) lay to rest the controversy over thermal bremsstrahlung and inverse Compton interpretations of the X-ray emission in our energy band. However, we do not rule out the presence of a power law component exceeding thermal emission above some energy, since such an inverse Compton component must exist at some level in those clusters with known radio emission.

There is also the question of whether the intracluster gas, believed by the above arguments to exist, is galactic or primordial. Iron lines, which imply approximately the same abundance relative to hydrogen in all clusters, are not easily explained unless part of the gas has been processed through stars, presumably in galaxies. Furthermore, interpretation of the correlation between the emission measure and the central galaxy density

is perhaps simpler if gas has come from the galaxies. It is satisfying to provide observational evidence for a galactic origin of intracluster gas, since theory has long predicted that galaxies in clusters should lose gas (Mathews and Baker 1971; Gunn and Gott 1972; Yahil and Ostriker 1973; Larson and Dinerstein 1975; Lea and DeYoung 1976).

However, the evidence that $kT \propto (\Delta v_c)^2$ and $kT \propto \bar{N}_o$ leaves little doubt that the cluster gas is in fact responding to the overall gravitational potential and does not have a temperature determined by the heat input of active galaxies or random explosive events. Thus it is perhaps puzzling that there seems to be strong evidence for an association between low frequency radio sources and cluster X-ray sources (Erickson, Mathews, and Viner 1977). Nevertheless, the facts may be brought into agreement, as shown recently by Lea and Holman (1977). These authors discuss the case in which relativistic electrons emit synchrotron radio flux but also heat intracluster gas, which then emits X-rays by thermal bremsstrahlung. Therefore, we conclude that some combination of the expected heating due to gravitational collapse and that due to nonthermal particles is responsible for the observed X-ray temperatures.

The role of dominant galaxies and cluster morphology in determining characteristics of the X-ray emission can be clarified somewhat by studying our correlations, although spatially resolved observations are bound to be more useful for this purpose (e.g. Gorenstein et al. 1977). First of all, we find that a kT vs. $(\Delta v_c)^2$ relation is tighter when cD clusters are omitted. This may be because cD galaxies are contributing enough X-ray flux to the overall cluster spectrum to upset our determination of

the temperature of the extended component. The contribution from a single galaxy component could appear either hotter or cooler than the extended component: hotter if some compact nonthermal emission source adds a power law component which exceeds the thermal emission above some energy, and cooler if the concentration of mass in a galaxy provides a site for particularly rapid cooling in an infall model such as that of Cowie and Binney (1977). Secondly, we found definite increases in kT and $\langle n_e n_H \rangle V$ when one progressed from irregular to centrally condensed clusters, as indicated by RS type. These correlations can be interpreted as indications that more centrally condensed clusters either: 1) produce more intracluster gas per unit virial mass; or 2) bring their gas into a more compact atmosphere so that their emission, which is proportional to n^2, is enhanced; or 3) some combination of 1) and 2). Of course, spatial observations have directly shown the possibility of compact components in several clusters: Virgo (Gorenstein et al. 1977), Perseus (Cash, Malina, and Wolff 1976), Centaurus (Mitchell et al. 1975), A478 (Schnopper et al. 1977), and A2319 (Grindlay et al. 1977). A particularly critical question relating to dominant or active galaxies is whether the iron line could arise within a single galaxy rather than in the extended component. Ulmer and Jernigan (1977) have attempted to answer this for Perseus, but their result has low significance. Having the iron lines come from single galaxies often requires large overabundances of iron in the galaxies (e.g. Gorenstein et al. 1977). But the best evidence that iron lines arise in the extended components is our finding that, when this is assumed, all the derived iron abundances are consistent with the same value.

The correlations and conclusions discussed above reflect both the utility and the limitations of the data we have used from the CXS experiment. Such parameters as the temperature, X-ray luminosity, and emission integral can be derived in a manner which is effectively experiment-independent, but which is still model-dependent. Since our fields of view integrate over these extended sources, we are unable to unambiguously define the detailed characteristics of realistic models of hot gas in clusters, although it is possible to achieve consistency with certain assumptions (e.g. constant iron abundance) and classes of models (e.g. polytropes). Complimentary observations at higher energies and observations with better spatial resolution are necessary to further define the applicable models.

After this paper was submitted for publication, a paper by Mitchell, Ives, and Culhane (1977) on X-ray clusters of galaxies appeared in print which discussed a similar body of data from Ariel 5. These authors reached several conclusions which are consistent with ours, and we will make a full comparison in the next paper of this series (Smith et al. 1978a).

R. F. Mushotzky and Barham W. Smith are grateful for the award of NAS/NRC Resdient Research Associateships for the period in which this work was done. We thank Steve Pravdo, Jean Swank, and Robert Becker for useful discussions.

REFERENCES

Abell, G. O. 1958, Ap. J. Suppl., 3, 211.

Avni, Y. 1976, Ap. J., 210, 642.

Bahcall, J. N., and Sarazin, C. L. 1977, Ap. J. (Letters), 213, L99.

Bahcall, N. A. 1975, Ap. J., 198, 249.

Bahcall, N. A. 1977a, Ap. J. (Letters), 217, L77.

Bahcall, N. A. 1977b, Ap. J. (Letters), in press.

Bhalla, C. P., Gabriel, A. H., and Presnyakov, L. P. 1975, M.N.R.A.S., 172, 359.

Boldt, E. A. 1977, Annals New York Academy of Sciences, in press.

Brown, R. L., and Gould, R. J. 1970, Phys. Rev., D1, 2252.

Cash, W., Malina, R. F., and Wolff, R. S. 1976, Ap. J. (Letters), 209, L111.

Chincarini, G., and Rood, H. J. 1971, Ap. J., 168, 321.

Cooke, B. A., Ricketts, M. J., Maccacaro, T., Pye, J. P., Elvis, M., Watson, M. G., Griffiths, R. E., Pounds, K. A., McHardy, I., Maccagni, D., Seward, F. D., Page, C. G., and Turner, M.J.L. 1977, M.N.R.A.S., in press.

Cowie, L. L., and Binney, J. 1977, Ap. J., 215, 723.

Culhane, J. L. 1977, Q.J.R.A.S., in press.

Erickson, W. C., Mathews, T. A., and Viner, M. R. 1977, submitted to Ap. J.

Faber, S. M., and Dressler, A. 1976a, Ap. J. (Letters) 210, L6r.

Faber, S. M., and Dressler, A. 1976b, Ap. J. 82, 187.

Fabian, A. C., Pringle, J. E., and Rees, M. 1976, Nature 263, 301.

Felten, J. E., and Morrison, P. 1966, Ap. J., 146, 686.

Fireman, E. L. 1974, Ap. J., 187, 57.

Forman, W., Jones, C., and Tananbaum, H. 1976, Ap. J. (Letters), 206, L29.

Forman, W., Jones, C., Cominsky, L., Julien, P., Murray, S., Peters, G., Tananbaum, H., and Giacconi, R. 1977, submitted to Ap. J. Suppl.

Gorenstein, P., Fabricant, D., Topka, K., Tucker, W., Harnden, F. R. 1977, Ap. J. (Letters), 216, L95.

Grindlay, J. E., Parsignault, D. R., Gursky, H., Brinkman, A. C., Heise, J., and Harris, D. E. 1977, Ap. J. (Letters), 214, L57.

Gunn, J. E., and Gott, J. R. 1972, Ap. J., 176, 1.

Gursky, H., Kellogg, E., Murray, S., Leong, C., Tananbaum, H., and Giacconi, R. 1971, Ap. J. 167, L81.

Gursky, H., and Schwartz, D. A. 1977, Ann. Rev. Astron. Ap., 15, in press.

Harris, D. E., and Romanshin, W. 1974, Ap. J., 188, 209.

Heiles, C. 1975, Astr. Ap. Suppl., 20, 37.

Hintzen, P., Scott, J. S., and Tarenghi, M. 1977, Ap. J., 212, 8.

Jones, C., and Forman, W. 1977, preprint.

Jones, M. 1974, M.N.R.A.S., 169, 211.

Katz, J. I. 1976, Ap. J., 207, 25.

Kellogg, E., Baldwin, J. R., and Koch, D. 1975, Ap. J., 199, 299.

Kellogg, E., and Murray, S. 1974, Ap. J. (Letters), 193, L57.

King, I. R. 1972, Ap. J. (Letters), 174, L123.

Lampton, M., Margon, B., and Bowyer, S. 1976, Ap. J., 208, 177.

Larson, R. B., and Dinerstein, H. L. 1975, P.A.S.P., 87, 911.

Lea, S. M. 1977, in Highlights of Astronomy, Vol. IV (Reidel), in press.

Lea, S. M., and DeYoung, D. S. 1976, Ap. J., 210, 647.

Lea, S. M., and Holman, G. D. 1977, preprint.

Leir, A. A., and van den Bergh, S. 1977, Ap. J. Suppl., 34, 381.

Lugger, P. 1977, submitted to Ap. J.

Malina, R. F., Lea, S. M., Lampton, M., Bowyer, C. S. 1977, preprint.

Mathews, W. G., and Baker, J. C. 1971, Ap. J., 179, 241.

Mewe, R. 1972, Astr. Ap., 20, 215.

Mitchell, R. J., Charles, P. A., Culhane, S. L., Davidson, P.J.N., and Fabian, A. C. 1975, Ap. J. (Letters), 200, L5.

Mitchell, R. J., and Culhane, J. L. 1977, M.N.R.A.S., 178, 75.

Mitchell, R. J., Culhane, J. L., Davison, P.J.N., and Ives, J. C. 1976, M.N.R.A.S., 176, 29.

Pravdo, S. H., Becker, R. H., Boldt, E. A., Holt, S. S., Rothschild, R. E., Serlemitsos, P. J., and Swank, J. H. 1977, Ap. J. (Letters), 206, L41.

Pravdo, S. H. 1977, Ph.D. Thesis, University of Maryland (NASA/GSFC Doc. X-661-76-280).

Raymond, J. C., and Smith, B. W. 1977, Ap. J. Suppl., in press.

Rood, H. J., Page, T. L., Kintner, E. C., and King, I. R. 1972, Ap. J., 175, 627.

Rood, H. J., and Sastry, G. N. 1971, P.A.S.P., 83, 313.

Ryter, C., Cesarsky, C. J., and Audouze, J. 1975, Ap. J., 198, 103.

Schnopper, H. W., Strom, R. G., and Harris, D. E. 1977, B.A.A.S., 9, 348.

Schwartz, D. A. 1977, submitted to Ap. J. (Letters).

Serlemitsos, P. J., Smith, B. W., Boldt, E. A., Holt, S. S., and Swank, J. H. 1977, Ap. J. (Letters), 211, L63.

Smith, B. W., Mushotzky, R. F., and Serlemitsos, P. J., 1978a, in preparation.

Smith, B. W., Serlemitsos, P. J., Mushotzky, R. F., Boldt, E. A., and Holt, S. S. 1978b, in preparation.

Spinrad, H. 1975, Ap. J. (Letters), 199, L1.

Summers, H. P. 1974, Internal Memorandum 367, Appleton Laboratory

Ulmer, M. P., and Jernigan, J. G. 1977, B.A.A.S., 9, 350.

Warwick, R. S., and Pye, J. P. 1978, M.N.R.A.S., in press.

Yahil, A., and Ostriker, J. P. 1973, Ap. J., 185, 787.

Yahil, A., and Vidal, N. V. 1977, Ap. J., 214, 347.

TABLE 1

COMPARISON OF METHODS OF REPRESENTING

ERROR LIMITS

Cluster Name	Errors in kT (keV)		
	One Parameter, 68% Confidence[1]	Three Parameter Joint Estimation	
		68% Confidence[2]	90% Confidence[3]
Centaurus	(+.4, -.4)	(+.5, -.4)	(+1.2, -.9)
A2147	(+.4, -.4)	(+1.0, -.7)	(+1.6, -1.2)
A2319	(+.7, -.7)	(+3.8, -2.6)	(+7.0, -4.0)

[1]Here we have fixed all parameters except kT at the values which give the minimum χ^2 for the three parameter fit, and varied kT until χ^2 increased by 1.

[2]kT was varied while reminimizing the other two parameters until χ^2 increased over its minimum value by 1.

[3]The procedure of Lampton et al. (1976) was followed for determining 90% confidence limits for three parameters.

TABLE 2

RESULTS OF SPECTRAL FITS

					THERMAL					NONTHERMAL		
Catalog	Source Position	Name	Detector	Exposure 10^5 cm^2-s	kT	$N_H(10^{21})$	E W.	E_ℓ	χ^2 min,dof	Photon Index	$N_H(10^{21})$	χ^2 min,dof
2A	0251+413	A347/ A396	A	12	$4.1^{+.8}_{-.7}$	< 1.3	$.68^{+.38}_{-.30}$	$6.6\ (6.9^{+4}_{-.3})$	1.78	$2.55^{+.09}_{-.10}$	8^{+25}_{-8}	2.08
2A	0255+132	A401	A C	15 10	$6.7^{+2.1}_{-1.3}$	12^{+12}_{-11}	$.18^{+.43}_{-.18}$	6.2	1.45	$2.35^{+.30}_{-31}$	29 ± 14	1.75
2A	0316+413	A426 (Perseus)	A B	37 28	$6.79^{+.15}_{-.13}$	3 2± .7	.40±.03	6.7 ± .1	2.4	---	---	---
3U	0446+44	3C129 cluster	A B C	11 6 3 10	$5.4^{+1.0}_{-.7}$	$6\ 1^{+5\ 4}_{-5.0}$	$.33^{+.32}_{-33}$	6 6 ± 35	.69	$2\ 47^{+.14}_{-.14}$	22^{+6}_{-5}	1.16
2A	0626-541	SC0627 -544	C	7.1	$6.3^{+3.7}_{-1.9}$	< 54	< .91	6.4	.90	$2.7^{+.35}_{-.3}$	< 27	1 0
2A	1033-27	A1060	C	4.5	$3\ 1^{+3.9}_{-1.4}$	< 63	$2.18^{+4.16}_{-1.68}$	6.6	.92	--	Not Done	--
3U	1144+19	A1367	A	16	$1\ 3^{+1.2}_{-.6}$	42^{+57}_{-33}	---	---	.88	4.3 ± 2	47	1.3
					$2.8^{+1.0}_{-0.6}$	---						
2A	1150+720	A1254?	A B	 22	$18.4^{+3.8}_{-2.5}$	$5.4^{+10.8}_{-5.4}$	<.28	6.4	1.21	$1.75^{+15}_{-.14}$	6^{+7}_{-6}	1.17
2A	1228+125	M87 (Virgo)	A	26	2.2 ± .2	∿ 2	1.1 ± .4	6.45	1.06*	---	---	---

3U	1247-41	Centaurus** (NGC4696?)	C	17	5.3 $^{+1.1}_{-.8}$	< 10	.41 $^{+.34}_{-.33}$	6.7 (6.45 ± .55)	96	2.65 $^{+.26}_{-.29}$	22 $^{+21}_{-22}$	1.27
3U	1252-28	SC1251 -288	C	23	9.4 $^{+2.7}_{-1.7}$	< 9	.53 $^{+.43}_{-.39}$	6.35 ± .2	74	2.21 $^{+.29}_{-.25}$	23 $^{+25}_{-23}$	1.11
2A	1257+283	A1656 (Coma)	A	17	8.85 $^{+1.05}_{-1.00}$	3.1 $^{+2.7}_{-2.3}$	32 $^{+.13}_{-.15}$	6.75 (7.05 $^{+.35}_{-.30}$)	1.72	---	---	---
2A	1326-311	SC1329 -314	B	5.0	8.2 $^{+7.3}_{-3.0}$	< 13	.45 $^{+.61}_{-.45}$	6.3	.77	1.92 $^{+.42}_{-.32}$	5.4 $^{+14}_{-5.4}$	.90
2A	1508+062	A2029	A	2.6	6.2 $^{+2.6}_{-1.6}$	< 7.7	12 $^{+.98}_{-.12}$	6.25	1.26	2.2 $^{+.6}_{-.3}$	2.7 $^{+24}_{-2.7}$	1.26
2A	1600+164	A2147 (Hercules)	A	15	7.2 $^{+1.4}_{-1.1}$	7.2 $^{+14.1}_{-7.2}$	< .55	6.5	53	2.14 $^{+.35}_{-.29}$	7.2 $^{+14}_{-7.2}$	.60
2A	1626+396	A2199	A	8.5	3.2 $^{+1.7}_{-1.0}$	< 17	.61 $^{+1.63}_{-.61}$	6.5	.74	3.05 $^{+.92}_{-.69}$	14 $^{+27}_{-14}$	.83
2A	1705+786	A2256	A	15	7.0 $^{+3.0}_{-2.0}$	< 13	.19 $^{+.68}_{-.19}$	6.3	.96	2.33 $^{+.47}_{-.36}$	13 $^{+18}_{-13}$	1.02
2A	1919+438	A2319	A	5.9	12.5 $^{+7.0}_{-4.0}$	3.2 $^{+7.9}_{-3.2}$	.26 $^{+.56}_{-.26}$	6.55	.98	1.69 $^{+.10}_{-.12}$	13 $^{+13}_{-9}$	1.19
2A	2322+166	A2589	A	29	9.0 $^{+12}_{-4.3}$	< 14	.57 $^{+1.32}_{-.57}$	6.6	.88	2.08 $^{+.55}_{-.42}$	9 $^{+20}_{-9}$	.87
3U	1555+27	A2142	A	19	53 $^{+\infty}_{-20}$	< 14	.43 $^{+.30}_{-.30}$	6.6 ± .3	1.13	1.37 $^{+.1}_{-.2}$	4.5 $^{+10.0}_{-4.5}$	1.56

*For best fitting 8 parameter model including line, absorption and two temperatures.

**The best fitting model indicates a definite excess of photons at E > 10 keV relative to a single temperature fit.

TABLE 3

OPTICAL AND RADIO CLUSTER DATA

NAME	z[1]	$N_H(10^{21})$	Δv[2]	$\bar{N}_o$[5]	Richness	RS[6]	F(Sp)[7]	α_{LFR}[8]
A347	.019	1-2	---	?	0	?	---	1.6
A401	.075	∿1	1390 ± 150	35	2	cD	---	1.64
A426	018	∿1.6	1396 ± 140	33	2	L	.09	.7 - 1.6
3C129	.022	∿3	---	---	?	?	---	.77 - 1.4
SC0627	∿.05	---	---	19	2	C	---	---
A1060	.011	1-2	771^{+116}_{-139}	13	1	C	.54	1.0
A1367	.022	0.16	847 ± 200	18	2	F	.40	1.4
A1254?	∿.05	0.6	---	?	2	?	---	---
Virgo	.0038	0.39	705 ± 48	11	1?	I	.55	.79
Cen	.011	---	945 ± 250	15	2	I	.45	1.13
SC1251	.056	0.61	---	25	3	cD	---	1.1
A1656	.023	0.28	900 ± 63	28	2	B	.13	1.3
SC1329	.073	0.5	---	?	3	cD	---	---
A2029	.078	0.39	1514^{+134}_{-272}[3]	32	2	cD	---	---
A2147	038	0.39	1120 ± 150	12	1	F (2Bb)	.27	.8 - 1.0
A2199	.031	0.16	843^{+110}_{-118}	19	2	cDp	.24	82
A2256	.055	0.61	1274^{+229}_{-280}	32	2	B	---	2.0
A2319	.054	0.83	873^{+131}_{-148}[4]	---	1	cD	---	1.2
A2589	.044	0.5	---	20	0	cD	.30	---

[1] Redshift data from Yahil and Vidal (1977), Bahcall (1977a), Lugger (1977), and Leir and van den Bergh (1977).

[2] Mean velocity dispersions from Faber and Dressler (1976a,b), Yahil and Vidal (1977), and Hintzen, Scott, and Tarenghi (1977).

[3] All objects included. $\Delta v = 788^{+229}_{-165}$ if some objects excluded (Faber and Dressler 1976b).

[4] Assuming X-ray source is A2319A. If A2319B is not separate, $\Delta v = 1627^{+195}_{-244}$ (Faber and Dressler 1976a,b).

[5] Central galaxy density (Bahcall 1977a).

[6] Cluster morphological type (Rood and Sastry 1971).

[7] Fraction of cluster galaxies which are spirals (Bahcall 1977b).

[8] Low frequency radio spectral index (Erickson, Matthews, and Viner 1977).

TABLE 4

CLUSTER LUMINOSITIES, EMISSION INTEGRALS AND FLUXES

Name	(1) Flux at 5 keV	(2) $\langle n_e n_H \rangle V$	(3) 2-6 keV Luminosity	(4) 2-10 keV Luminosity	(5) Bolometric Luminosity
A347/396	1.9	3.3	1.52	1.98	5.02
A401	1.1	22.0	13.9	21.90	43.2
A426	13.6	14.0	8.44	12.40	28.0
3C129	1.7	3.7	1.88	2.73	6.55
3C0626	1.02	9.4	5.98	8.40	18.0
A1367	0.29	(1.05-7.4)[1]	0.45	.54	(1.33-6.6)[1]
A1254	1.6	10.3	4.90	6.25	21.7
Virgo	5.72	0.63	0.234	.289	.655
Cen	1.6	0.87	0.51	.71	1.54
A1656	5.5	9.3	4.87	7.6	16.6
3C1251	1.5	12.0	8.30	13.0	27.9
3C1329	1.75	31.0	21.1	31.0	66.7
A2029	1.50	27.0	17.0	23.7	50.8
A2147	.97	3.6	2.39	3.44	7.33
A2199	.66	3.5	1.48	1.82	4.74
A2256	.95	9.6	6.22	8.93	19.3
A2319	2.10	13.8	9.80	15.7	36.7
A2589	.56	2.8	1.96	2.97	6.28
A2142	1.85	---[2]	21.2	34.7	---[2]

Col. 1 units are 10^{-11} ergs/cm^{2}sec keV; Col. 2 units are 10^{67} cm^{-3}; Col. 3,4,5 units are 10^{44} ergs/sec using measured or estimated (A1254,2142) (Leir and van den Bergh 1977) redshift of cluster and H_o = 50 km sec^{-1} Mpc^{-1}.

Notes To Table. (1) for A1367 value depends on whether kT = 1.3 or kT = 2.8.

(2) due only to lower kT limit L_{BOL} or $\langle n_e n_H \rangle V$ cannot be calculated exactly.

TABLE 5

WEAK DETECTIONS AND UPPER LIMITS

Source Position	Name	OSO-8* 2-6 keV	OSO-8* 2-10 keV	4U Counts 2-6 keV	2A Counts 2-10 keV	Comment
4U0037-10	A85	2.3 ± .2	1.3 ± .2	2.9 ± .3	1.2 ± .1	kT > 10 keV ?
2A0102-222/ 2A0102-242	A140/ A133	1.7 ± .2	1.2 ± .2	5.8 ± 1.1	0.7 ± .2	kT > 10 keV ?
4U0148+36	A262	2.3 ± .7	0.9 ± .3	2.4 ± .8	< .73	2.2 < kT < 7.2 keV (1σ limits)
2A0815-075	A644	< 2.2	< .85	----	0.8 ± .1	2σ upper limits
4U1636+05	A2204	< 1.3	< .45	3.6 ± .6	0.3 ± .1	2σ upper limits
3U2346+26	A2666	2.35 ± .3	1.35 ± .15	2.44 ± .4	< .63	kT > 10 keV ?

*We report our 2-6 keV flux in units of 1.7×10^{-11} erg cm^{-2} s^{-1} and our 2-10 keV flux in units of 5.1×10^{-11} erg cm^{-2} s^{-1} to facilitate comparison with fluxes from the 4U and 2A catalogs expressed in counts.

FIGURE CAPTIONS

Figure 1a. Photon spectra derived from CXS pulse height data for four clusters in which iron line features at $\sim$ 6.7 keV are found with 90% confidence. 1σ error bars from counting statistics alone are shown.

Figure 1b. Photon spectra for four sources in which iron lines are not found with 90% confidence. Note that counting statistics are in general poorer than in Fig. 1a, and that some of these sources show evidence for iron lines at lower significance.

Figure 2. The upper portion shows the equivalent width (E.W.) as a function of temperature. Solid line: Predicted E.W. for Fe/H = 2.6×10^{-5} by number, from Raymond and Smith (1977) Dashed line: Same, for Fe/H = 1.4×10^{-5}. Data points with 90% confidence error bars are plotted for seven clusters. The lower portion of the figure shows derived values of Fe/H for most of the clusters in our sample. All points except Virgo, and all upper limits, are consistent with the Perseus value, Fe/H = $(1.4 \pm .1) \times 10^{-5}$.

Figure 3. Light curves for single observations of the 3C129 cluster and Abell 2589. The ordinate is the total 2 - 60 keV flux, and 1σ error bars from counting statistics alone are shown. Errors generally increase when the source moves off axis, and gaps in the data are due to various causes.

Figure 4. Flux measured by OSO-8 vs. (a) 3U, (b) 4U, and (c) 2A fluxes. Both OSO-8 and UHURU fluxes are express in units of 1.7×10^{-11} erg cm^{-2} s^{-1} keV^{-1} in (a) and (b). In (c) both OSO-8 and Ariel 5 fluxes are in units of 5.1×10^{-11} erg cm^{-2} s^{-1} keV^{-1}. The point labeled (1) in (a) and (b) is Abell 1367, and (2) is Abell 2589. Errors in OSO-8 fluxes are estimated systematic uncertainties, typically 10%.

Figure 5. Optically measured central velocity dispersion of the galaxies vs. OSO-8 measured X-ray temperatures. Errors in Δv_c are generally as quoted by optical observers, and those in kT are 90% confidence. Clusters with Rood-Sastry types cD and B are distinguished from the others. The velocity dispersions for Abell 2029 and Abell 2319 have two possible values (see Table 3). The dot-dash line is the best $kT \propto (\Delta v_c)^2$ fit to all data points.

Figure 6. X-ray temperature vs. bremsstrahlung emission integral for most of the clusters in our sample. Errors in $\langle n_e n_H \rangle V$ are the convolution of 90% confidence limits on kT and estimated errors of 10% on flux, while errors in kT are 90% confidence. The inclusion of absorption in Abell 1367 implies a significantly lower luminosity. The solid line is discussed in the text.

Figure 7. Central galaxy density ($\bar{N}_o$), in galaxies per π (0.5 Mpc)^2 as measured by Bahcall (1977a), vs. X-ray temperature. Errors in $\bar{N}_o$ are $\pm$ 20% as estimated by Bahcall.

Figure 8. Central galaxy density ($\bar{N}_o$), richness class (R), and Rood-Sastry type (RS) vs. bremsstrahlung emission integral ($\langle n_e n_H \rangle$ V) as derived from CXS data. The richness correlation is the weakest of the three.

Figure 9. The fraction of cluster galaxies classified as spirals, F(Sp), as given by Bahcall (1977b), vs. ($\langle n_e n_H \rangle$ V)$^{\frac{1}{2}}$ kT, a possible measure of the ram pressure experienced by galaxies moving through intracluster gas at the center of a cluster.

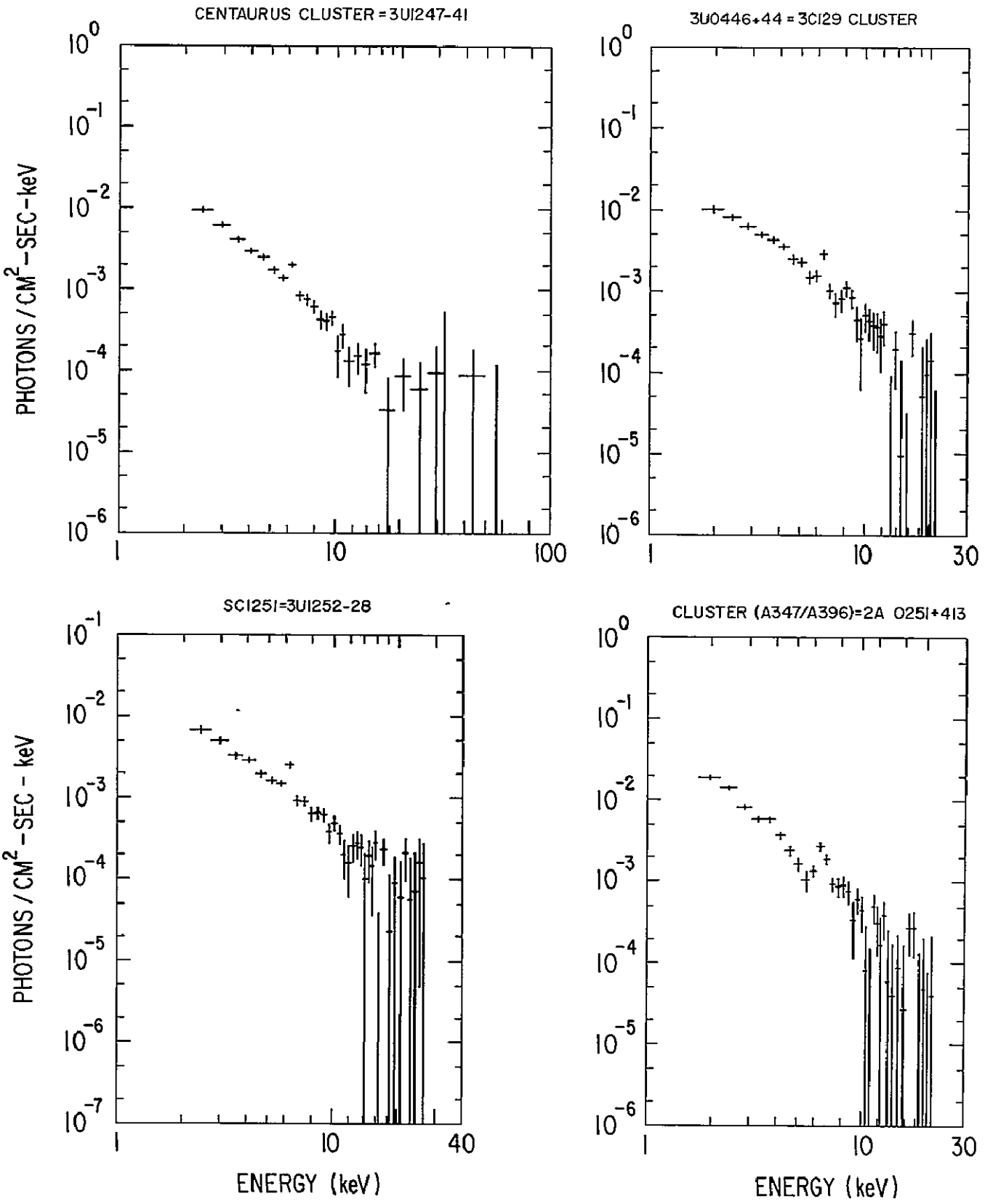

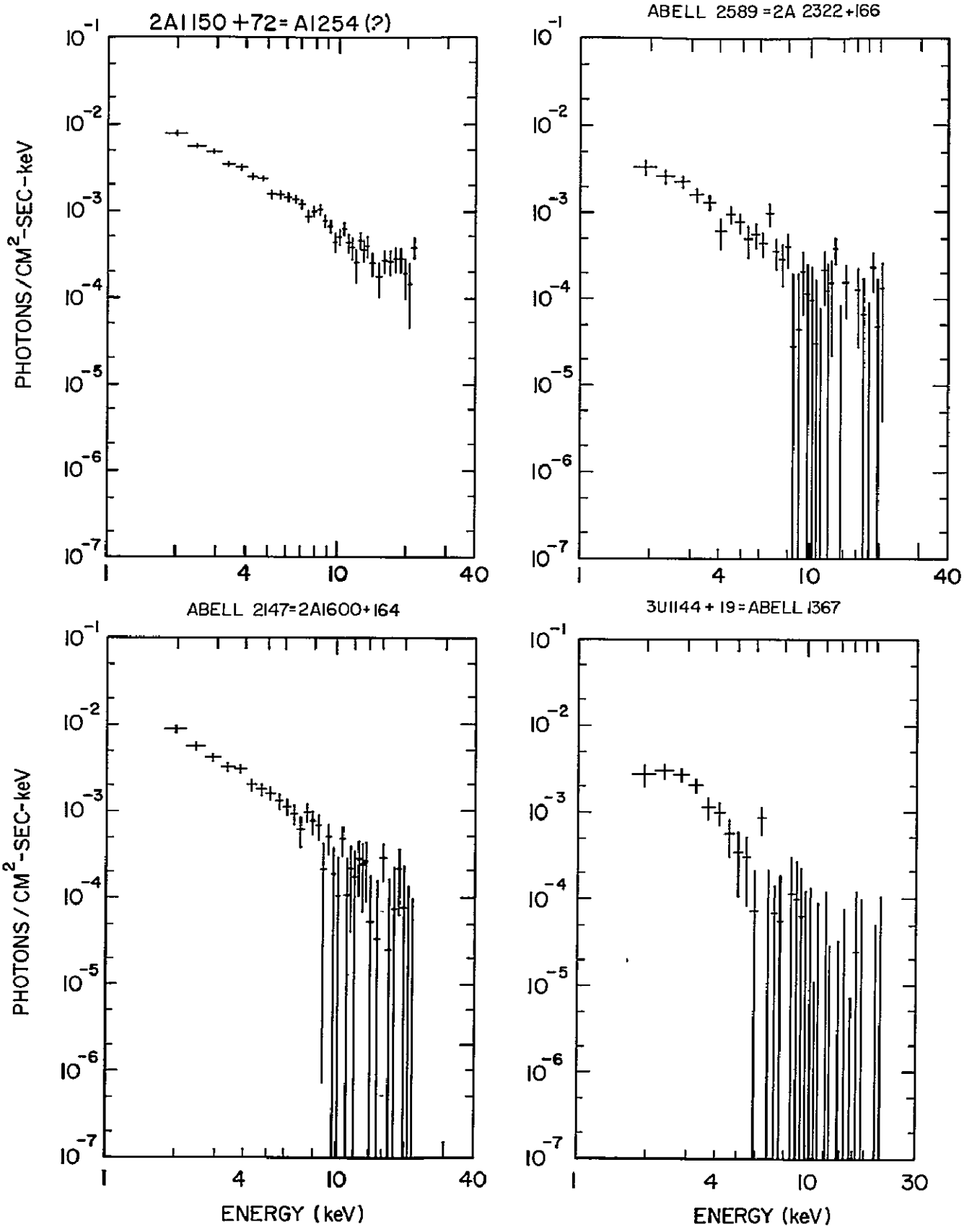
2A1150+72=A1254 (?)
ABELL 2589=2A 2322+166
ABELL 2147=2A1600+164
3U1144+19=ABELL 1367
PHOTONS/CM²-SEC-keV
ENERGY (keV)
1
4
10
40
30

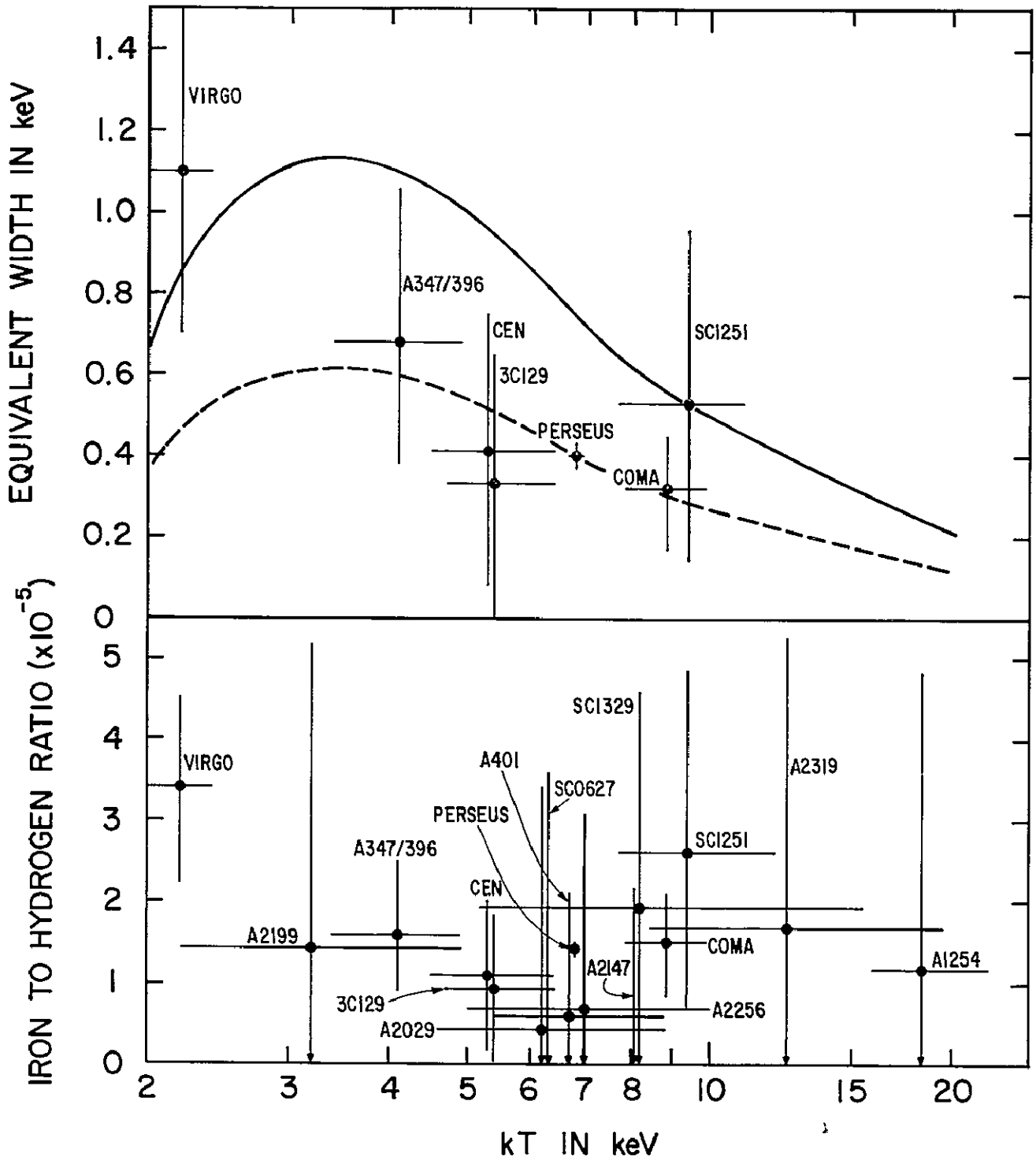

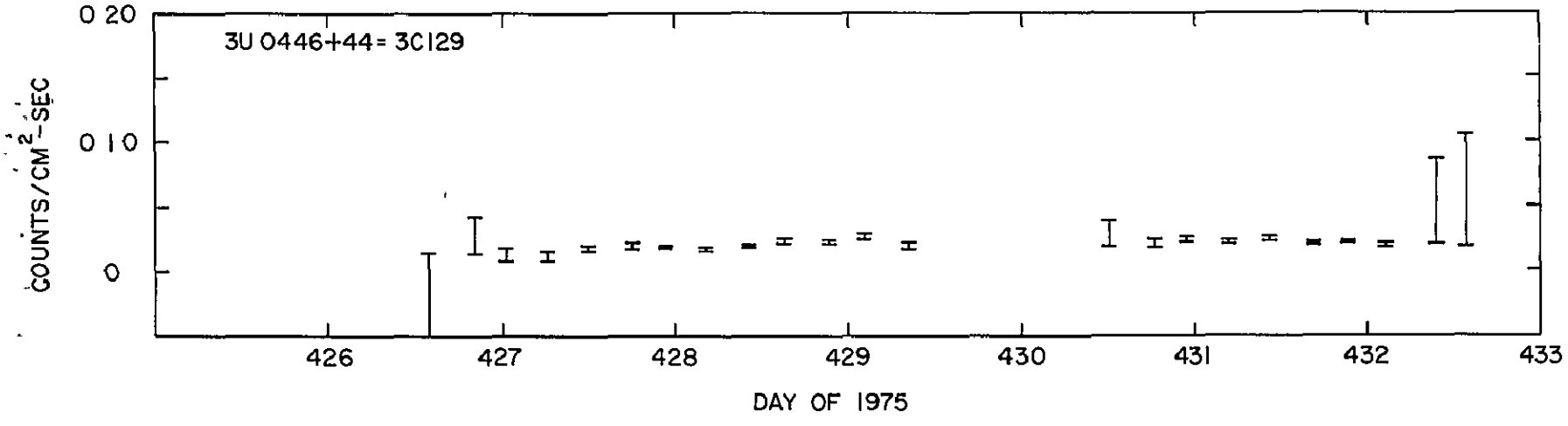
3U 0446+44 = 3C129
0 20
0 10
0
COUNTS/CM^2-SEC
426
427
428
429
430
431
432
433
DAY OF 1975

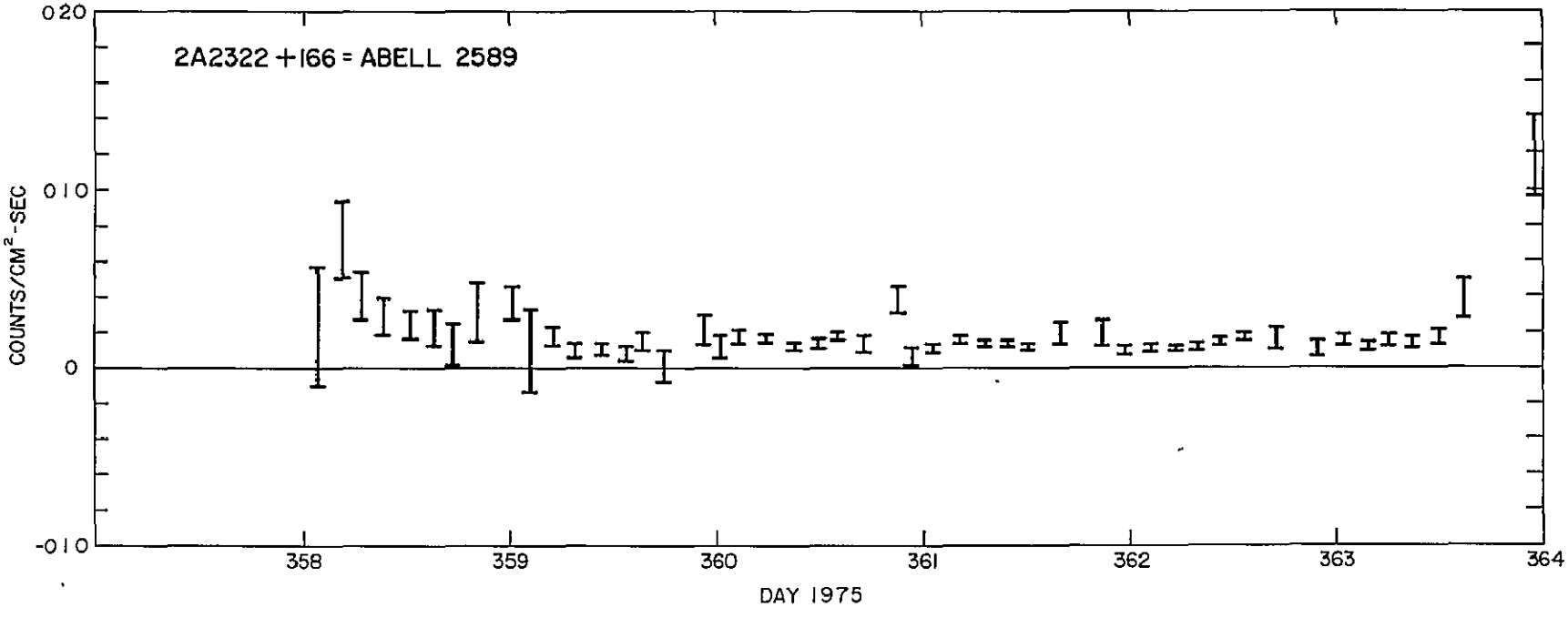
2A2322 +166 = ABELL 2589
020
010
0
-010
COUNTS/CM^2-SEC
358
359
360
361
362
363
364
DAY 1975

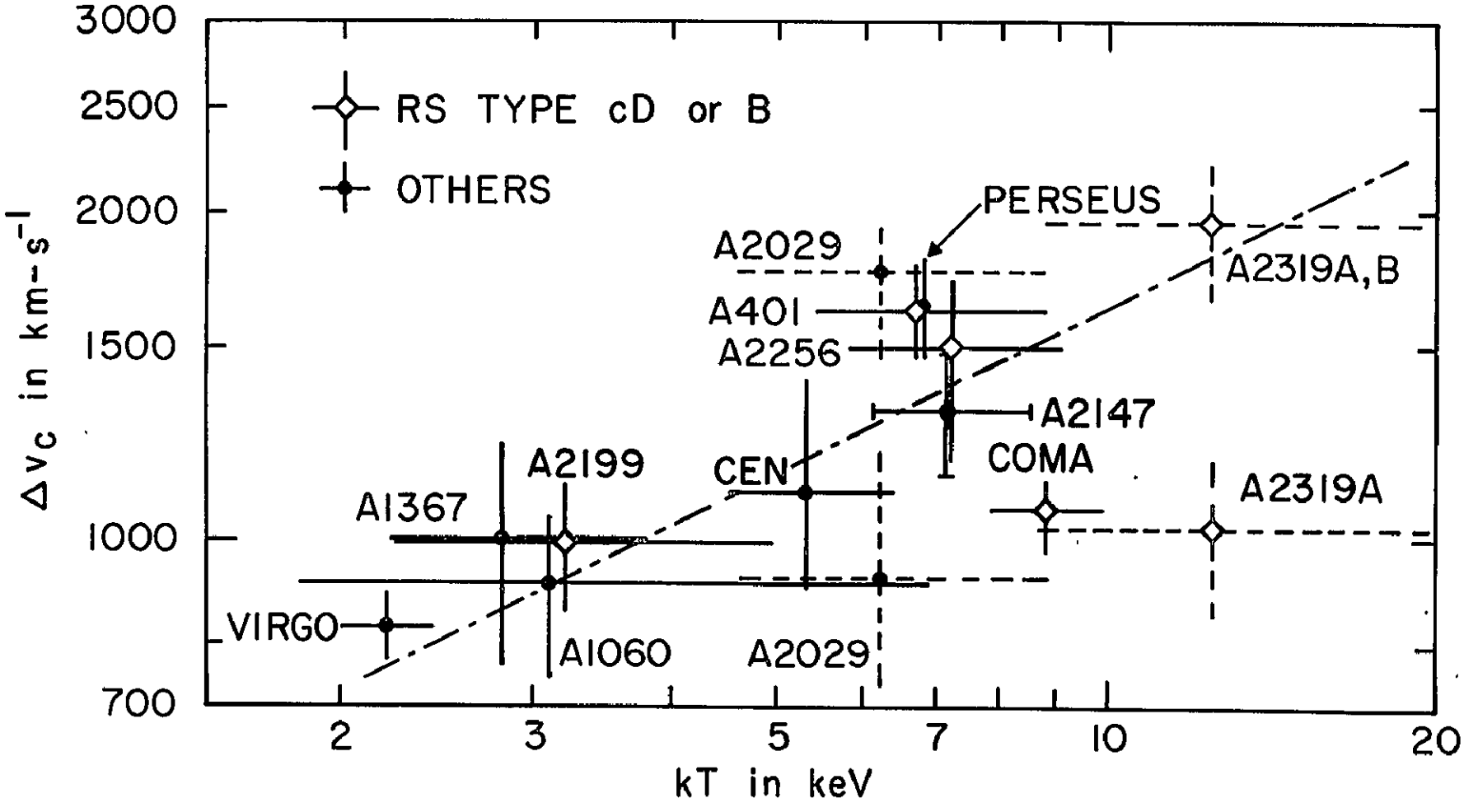
3000
2500
2000
1500
1000
700
Δv_c in km-s^{-1}
RS TYPE cD or B
OTHERS
PERSEUS
A2029
A2319A,B
A401
A2256
A2147
COMA
A2319A
CEN
A2199
A1367
VIRGO
A1060
A2029
2
3
5
7
10
20
kT in keV

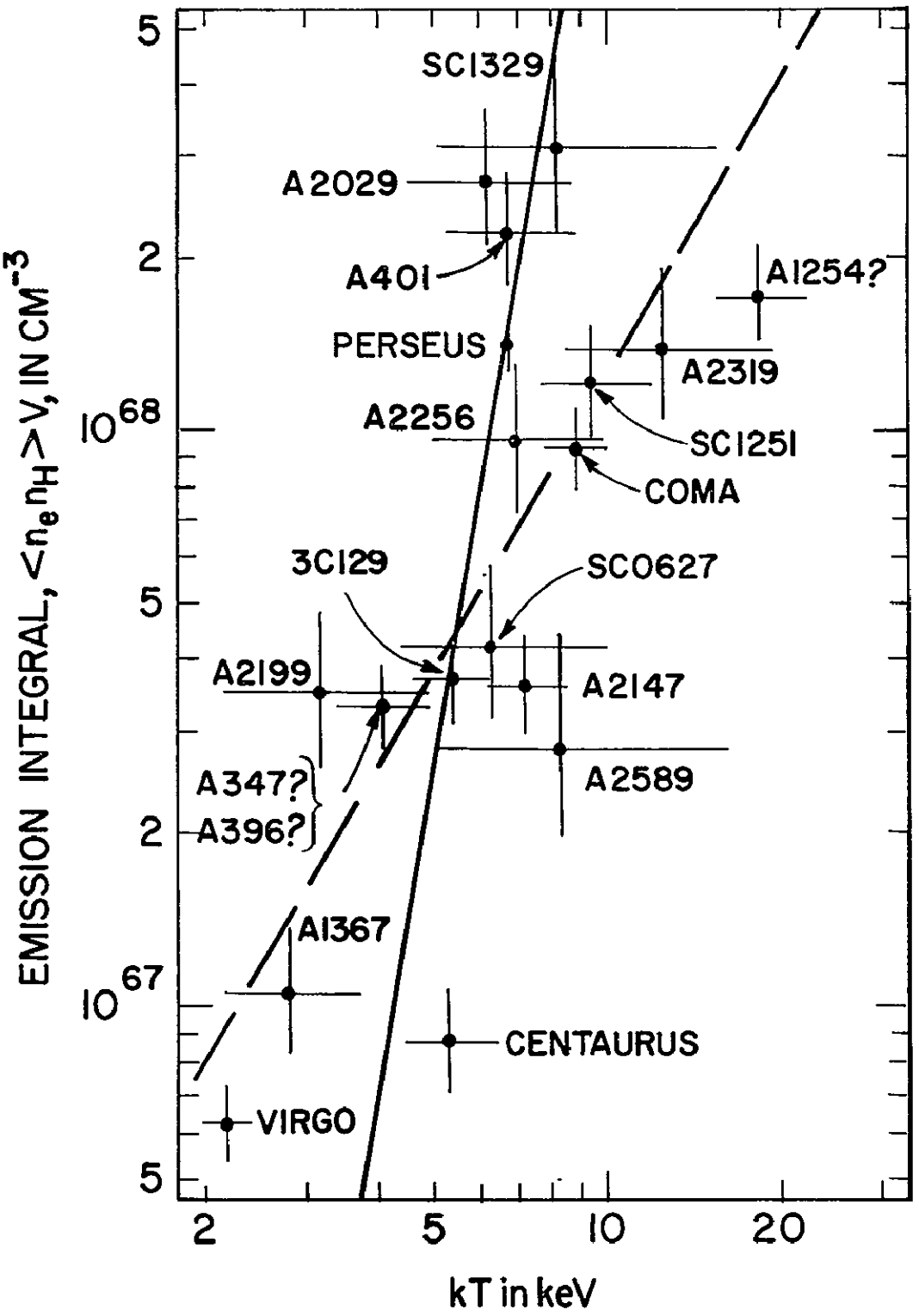

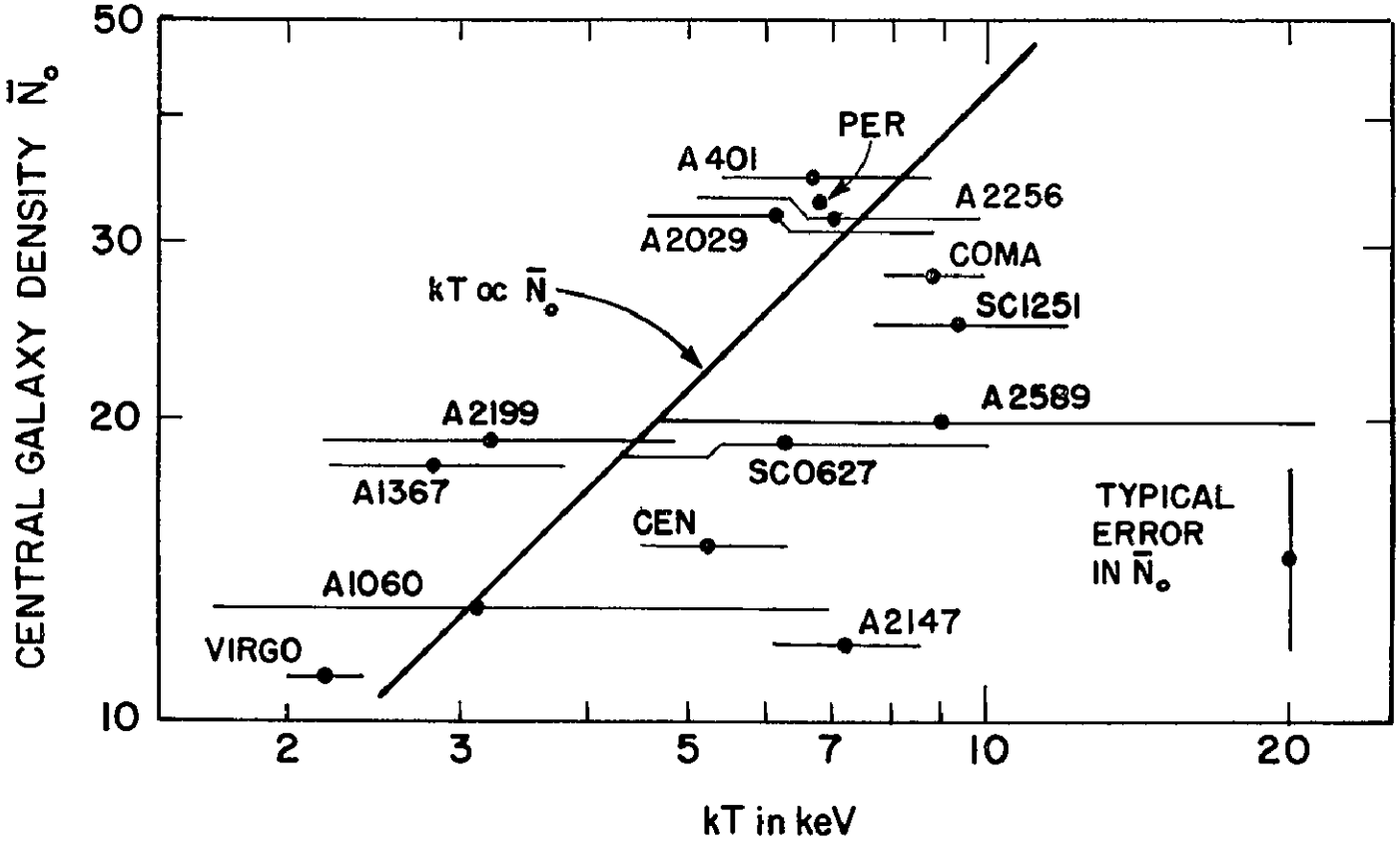
CENTRAL GALAXY DENSITY $\bar{N}_o$
50
30
20
10
2
3
5
7
10
20
kT in keV
PER
A401
A2256
A2029
COMA
SC1251
kT ∝ $\bar{N}_o$
A2589
A2199
SC0627
A1367
CEN
TYPICAL ERROR IN $\bar{N}_o$
A1060
A2147
VIRGO

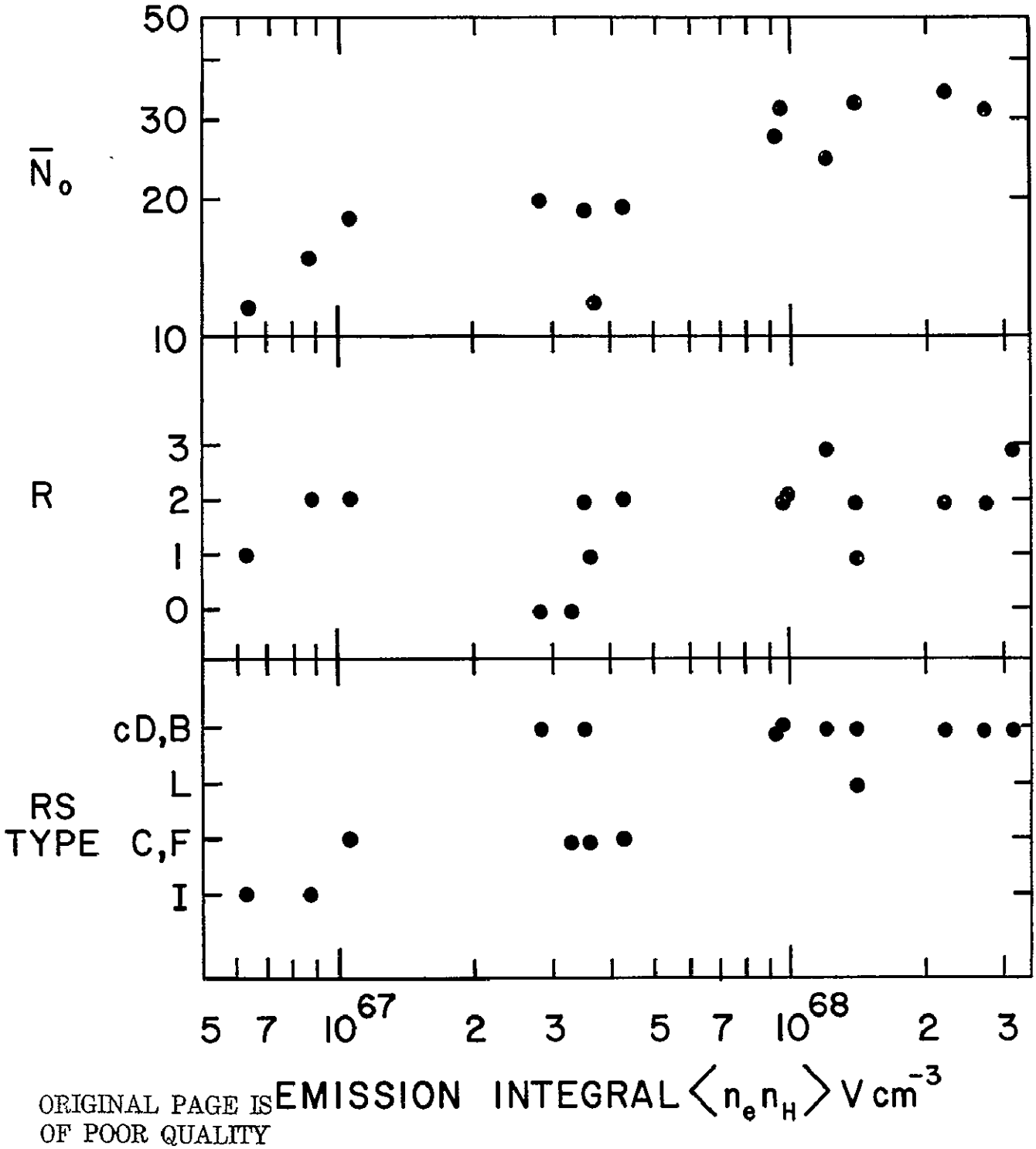

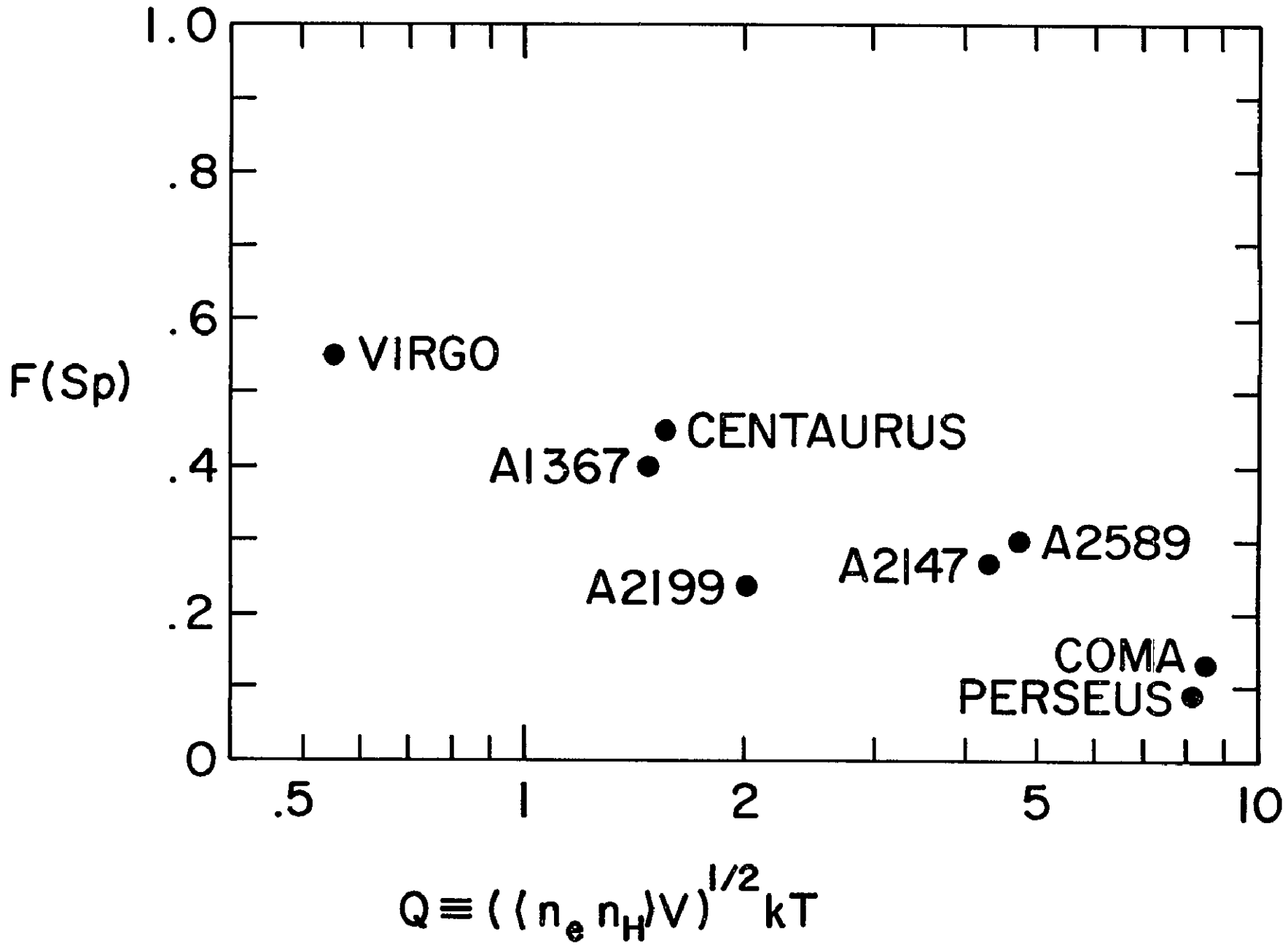
1.0
.8
.6
.4
.2
0
F(Sp)
VIRGO
CENTAURUS
A1367
A2199
A2147
A2589
COMA
PERSEUS
.5
1
2
5
10
$Q \equiv ((n_e n_H)V)^{1/2} kT$

BIBLIOGRAPHIC DATA SHEET

1 Report No	2. Government Accession No	3. Recipient's Catalog No
TM 78097		

4 Title and Subtitle	5. Report Date
OSO-8 X-RAY SPECTRA OF CLUSTERS OF GALAXIES. I. OBSERVATIONS OF TWENTY CLUSTERS: PHYSICAL CORRELATIONS	March 1978
	6. Performing Organization Code 661
7. Author(s) R.F. Mushotzky (NAS/NRC), P.J. Serlemitsos, B.W. Smith (U. of Md.), E.A. Boldt, S.S. Holt	8. Performing Organization Report No.
9 Performing Organization Name and Address Cosmic Radiations Branch Laboratory for High Energy Astrophysics Code 661	10 Work Unit No.
	11 Contract or Grant No.
	13 Type of Report and Period Covered TM
12 Sponsoring Agency Name and Address	14 Sponsoring Agency Code

15. Supplementary Notes

To be published in the Astrophysical Journal

16. Abstract

OSO-8 X-ray spectra from 2 to 20 keV have been analyzed for 26 clusters of galaxies. For 20 clusters we present temperatures, emission integrals, iron abundances, and low energy absorption measurements. Our data give, in general, better fits to thermal bremsstrahlung than to power law models. Eight clusters have positive iron emission line detections at the 90% confidence level, and all twenty cluster spectra are consistent with Fe/H = 1.4×10^{-5} by number with the possible exception of Virgo. Thus we confirm that X-ray emission in our energy band is predominantly thermal radiation from hot intracluster gas rather than inverse Compton radiation.

17. Key Words (Selected by Author(s))	18 Distribution Statement

19 Security Classif. (of this report)	20 Security Classif. (of this page)	21 No. of Pages	22 Price*
U	U	55	

*For sale by the National Technical Information Service, Springfield, Virginia 22151